Impact of Hall Current and Ion slip on a hybrid nanofluid flow with non-uniform source/sink

Thesis Submitted By

Maryam Afsar

01-248192-004

SUPERVISED BY

Prof. Dr. M. Ramzan

A dissertation submitted in fulfillment of the requirements for the award of the degree of MS (Mathematics)

Department of Computer Science

Bahria University Islamabad Campus

Session (2019-2021)

Bahria University
Discovering Knowledge

MS-13

Thesis Completion Certificate

Scholar's Name**:** **Maryam Afsar** Registration No: **63118** Program of Study: **MS Mathematics**
Thesis Title: **Impact of Hall Current and Ion slip on a hybrid nanofluid flow with non-uniform source/sink.**

It is to certify that the above student's thesis has been completed to my satisfaction and to my belief, its standard is appropriate for submission for Evaluation. I have also conducted plagiarism test of this theses using HEC prescribed software and found similarity index at 18% that is within the permissible limit set by the HEC for the MS/MPhil degree thesis. I have also found the thesis in a format recognized by the BU for MS/MPhil thesis.

Principal Supervisor's Signature: _____

Date: 16-10-2021 **Name: Prof. Dr. M. Ramzan**

Bahria University
Discovering Knowledge

MS-14A

Author's Declaration

I, **Maryam Afsar** hereby state that my MS thesis titled "**Impact of Hall Current and Ion slip on a hybrid nanofluid flow with non-uniform source/sink**" is my own work and has not been submitted previously by me for taking any degree from Bahria University, Islamabad or anywhere else in the country/abroad.

At any time if my statement is found to be incorrect even after my Graduation, the University has the right to withdraw my MS Degree.

Name of student: **Maryam Afsar**

Date: **15-10-2021**

Bahria University
Discovering Knowledge

MS-14B

Plagiarism Undertaking

I, solemnly declare that research work presented in thesis titled "**Impact of Hall Current and Ion slip on a hybrid nanofluid flow with non-uniform source/sink**" is solely my research work with no significant contribution from any other person. Small contribution/ help wherever takenhas been duly acknowledged and that complete thesis has been written by me.

I understand the zero tolerance policy of the HEC and Bahria University towards plagiarism. Therefore, I as an Author of above titled declare that no portion of my thesis has been plagiarized and any material used as references is properly referred/cited.

I understand that if I am found guilty of any formal plagiarism in the above titled thesis even after award of MS degree, the university reserved the right to withdraw/revoke my MS degree and that HEC and the University has the right to publish my name on the HEC/University website on which names of students are placed who submitted plagiarized thesis.

Student/ Author's Sign: _____

Name of the Student: **Maryam Afsar**

Dedicated to my beloved parents, husband and teachers whose tremendous support and cooperation led me to this wonderful accomplishment

Acknowledgments

I am thankful to Almighty ALLAH Who has enabled me to learn and to achieve milestones towards my destination and His beloved Prophet Hazrat Muhammad (ﷺ) Who is forever a constant source of guidance, a source of knowledge and blessing for entire creation. His teachings show us a way to live with dignity, stand with honor and learn to be humble.

My acknowledgment is to my kind, diligent and highly zealous supervisor, Prof. Dr. M. Ramzan, who supported me with his cherished opinions and inspirational discussions. His valuable expertise, comments, suggestions and instructions are most welcome that greatly improved the clarity of this document. I am placing my earnest thanks to Prof. Dr. M. Ramzan. I am so grateful to work under the supervision of such a great person.

My gratitude is to my honorable professors who took me to the apex of my academia with their guidance. In particular, Prof. Dr. Rizwan and Dr. Jafar Hasnain who have always been supportive in all of my course work and kept encouraging me throughout the session in Bahria University, Islamabad Campus. They are the true teachers who have made Mathematics Department of BUIC, a real place of learning.

My intense recognition is to my parents, my husband and adored siblings (for everything) who are always real pillars for my encouragement and showered their everlasting love, care and support throughout my life. Humble prayers, continuing support and encouragement of my family are as always highly appreciated. I also appreciate the moral support of all my friends, Maryam and Maham, especially Nazia Shahmir and all PhD scholars who did cooperation up to his best and help me at every step and stage at my research work. Consequently, my all plea is to Allah, the Almighty, the beneficent Whose blessings are always showered upon me via strengthening my wisdom and bestowed me with the knowledge of what he wants.

Maryam Afsar

Bahria University Islamabad, Pakistan

October 2021

Abstract

The current research scrutinizes the effects of Hall current and Ion slip impacts on a steady three-dimensional flow of hybrid nanofluid induced by bi-directional sheet stretching. Zinc oxide (ZnO) and Gold (Au) nanoparticles are dispersed in Kerosine oil and water to establish the two different hybrid nanofluids. Additionally, for heat transfer analysis, the temperature equation incorporates the effects of Cattaneo-Christov (C-C) heat flux and non-uniform heat source/sink. The Tiwari and Das model is used to examine the characteristics of the fluid flow. The similarity transformations are employed to reduce highly nonlinear governing partial differential equations to a system of ordinary differential equations and are numerically performed through the use of the MATLAB software's bvp4c scheme. Graphs are portrayed to demonstrate the effects of dimensionless parameters on the velocity and temperature fields. In addition, the skin friction coefficient and Nusselt number for practical applications are evaluated in Tabular form. It is learned that ZnO-Au/Kerosene Oil leads ZnO-Au/Water when it comes to temperature profile increase.

TABLE OF CONTENTS

CHAPTER	TITLE	PAGE
DECLARATION		**ii**
DEDICATION		**iii**
ACKNOWLEDGEMENTS		**iv**
ABSTRACT		**v**
TABLE OF CONTENTS		**vi**
LIST OF TABLES		**x**
LIST OF FIGURES		**xi**
NOMENCLATURE		**xiii**
1.	**Introduction and Literature review**	1
	1.1 Introduction	1
	1.2 Literature review	3
2.	**Preliminaries**	7
	2.1 Fluid	7
	2.2 Nanofluid	7
	2.3 Hybrid Nanofluid	7
	2.4 Fluid Mechanics	8
	2.4.1 Fluid Statics	8
	2.4.2 Fluid Dynamics	8
	2.5 Stress	8
	2.5.1 Shear stress	8

2.5.2 Normal Stress 9

2.6 Strain 9

2.7 Flow 9

2.6.1 Laminar Flow 9

2.6.2 Turbulent Flow 9

2.8 Viscosity 9

2.8.1 Dynamic Viscosity 10

2.8.2 Kinematic Visocsity 10

2.9 Newton’s law of viscosity 10

2.9.1 Newtonian Fluids 10

2.9.2 Non-Newtonian fluids 11

2.10 Density 12

2.11 Pressure 12

2.12 Mechanism of heat transfer 12

2.12.1 Conduction 12

2.12.2 Convection 13

2.12.3 Radiation 13

2.13 Dimensionless Numbers 14

2.13.1 Reynolds number 14

2.13.2 Prandtl number 14

2.13.3 Skin friction coefficient 14

2.13.4 Nusselt number 15

2.14 Fundamental laws 15

2.14.1 Law of mass conservation 16

2.14.2 Momentum conservation 16

2.14.3 Energy conservation 16

2.14.4 Conservation concentration 17

2.14.5 Thermal diffusivity 17

2.14.6 Thermal conductivity 17

2.15 Hall effect 18

3. Comparative analysis of magnetized partially ionized Copper, Copper Oxide-water and kerosene oil nanofluid flow with Cattaneo-Christov heat flux. 19

3.1 Mathematical formulation 20

3.2 Similarity Transformation 21

3.3 Results and Discussion 24

4. Impact of Hall Current and Ion slip on a hybrid nanofluid flow with non-uniform source/sink 36

4.1 Mathematical formulation 36

4.1.1 Governing Equations 39

4.1.2 Similarity Transformation 40

4.2 Numerical solution 42

4.3 Results and Discussion 43

5. Conclusions and future work **55**

5.2 Chapter 4 56

5.3 Chapter 5 56

Bibliography 57

LIST OF TABLES

Table NO.	TABLE	PAGE
Table 3.1(a)	Analysis of drag force in x-direction for water in Cu and CuO	30
Table 3.1(b)	Analysis of drag force in x-direction for kerosene oil in Cu and CuO	31
Table 3.2(a)	Analysis of drag force in y-direction for water in Cu and CuO	32
Table 3.2(b)	Analysis of drag force in y-direction for kerosene oil in Cu and CuO	33
Table 3.3(a)	Rate of heat transfer analysis for water in Cu and CuO	34
Table 3.3(b)	Rate of heat transfer analysis for kerosene oil in Cu and CuO	35
Table 4.1	Analysis of drag force in x-direction for water in ZnO and Au	53
Table 4.2	Analysis of drag force in y-direction for water in ZnO and Au	54
Table 4.3	Rate of heat transfer analysis for water and kerosene oil in ZnO and Au	55

LIST OF FIGURES

Figure No.	Title	Page No.
Figure 3.1	Stretching sheet framework	20
Figure 3.2	*Change in* $f'(\eta)$ vs. a	26
Figure 3.3	*Change in* $g'(\eta)$ *vs.* a	26
Figure 3.4	*Change in* $f'(\eta)$ *vs.* β_e	27
Figure 3.5	*Change in* $g'(\eta)$ *vs.* β_e	27
Figure 3.6	*Change in* $f'(\eta)$ *vs.* β_i	28
Figure 3.7	*Change in* $g'(\eta)$ *vs.* β_i	28
Figure 3.8	*Change in* $\theta(\eta)$ *vs.* a	29
Figure 3.9	*Change in* $\theta(\eta)$ *vs.* γ	29
Figure 4.1	Stretching sheet framework	37
Figure 4.2	*Change in* $f'(\eta)$ *vs.* a	45
Figure 4.3	*Change in* $g'(\eta)$ *vs.* a	45
Figure 4.4	*Change in* $f'(\eta)$ *vs.* β_e	46

Figure 4.5	*Change in* $g'(\eta)$ *vs.* β_e	46
Figure 4.6	*Change in* $f'(\eta)$ *vs.* β_i	47
Figure 4.7	*Change in* $g'(\eta)$ *vs.* β_i	47
Figure 4.8	*Change in* $\theta(\eta)$ *vs.* a	48
Figure 4.9	*Change in* $\theta(\eta)$ *vs.* β_e	48
Figure 4.10	*Change in* $\theta(\eta)$ *vs.* β_i	49
Figure 4.11	*Change in* $\theta(\eta)$ *vs.* γ	49
Figure 4.12	*Change in* $\theta(\eta)$ *vs.* ϕ	50
Figure 4.13	*Change in* $\theta(\eta)$ *vs.* A_1	50
Figure 4.14	*Change in* $\theta(\eta)$ vs. B_2	51

NOMENCLATURE

Acronyms	Description
CC	Cattaneo-Christov
Nu_x	Local Nusselt number
Symbols	
b, c	Positive dimensional constants
C_x	Skin friction coefficient in the x-direction (Dimensionless)
C_y	Skin friction coefficient in the y-direction (Dimensionless)
C_p	Specific heat capacity $(\mathrm{Jkg^{-1}K^{-1}})$
$(C_p)_f$	Specific heat capacity of fluid (--)
$(C_p)_{nf}$	Specific heat capacity of nanofluid (--)
$(C_p)_n$	Specific heat capacity of nanoparticles (--)
$f'(\eta)$	Dimensionless velocity in the *x*-direction
$\mathrm{g}'(\eta)$	Dimensionless velocity in the *y*-direction
Ha	Hartmann number (Dimensionless)
Pr	Prandtl number (Dimensionless)
k	Thermal conductivity $(\mathrm{WK^{-1}m^{-1}})$
k_n	Thermal conductivity of nanoparticles (--)
k_f	Thermal conductivity of fluid (--)
k_{nf}	Thermal conductivity of nanofluid (--)
$\mathrm{Re}_{x_L}, \mathrm{Re}_{y_L}$	Local Reynolds number in x and y-direction (Dimensionless)
T	Temperature (K)
T_w	Temperature of surface (--)
u, v, w	Components of Velocity in x-, y-, z-directions $(\mathrm{ms^{-1}})$
x, y, z	Axis coordinates (m)
q_w	Heat flux near the wall
q	Heat flux vector
J	Current density vector
B	Magnetic induction vector
E	Electric induction vector

Greek Symbols	
$\theta(\eta)$	Dimensionless temperature
η	Similarity transformation variable (Dimensionless)
ρ	Density (kgm^{-3})
ρ_n	Density of nanoparticles (--)
ρ_f	Density of fluid (--)
ρ_{nf}	Density of nanofluid (--)
μ	Dynamic viscosity $(kgm^{-1}s^{-1})$
μ_f	Fluid dynamic viscosity (--)
μ_{nf}	Nanofluid dynamic viscosity (--)
ϕ	Volume fraction of nanoparticles (molL^{-1})
σ_f	Electrical conductivity of fluid $(kgm^{-3}s^3A^2)$
σ_{nf}	Nanofluid electrical conductivity (--)
α_{nf}	Thermal diffusivity of nanofluid
τ_{zx}, τ_{zy}	Shear stress near *x*- and *y*- directions
ν	Kinematic viscosity (m^2s^{-1})
ν_f	Kinematic viscosity of the fluid (--)
ν_{nf}	Nanofluid kinematic viscosity (--)
τ_0	Thermal relaxation characteristic time $(\succ 0)$
γ	Thermal relaxation coefficient (Dimensionless)
β_e	Hall parameter (Dimensionless)
β_i	Ion slip parameter (Dimensionless)
Q	Non-uniform source/sink
Subscripts	
∞	Use for ambient
w	For wall surface
nf	Nanofluid
hnf	Hybrid nanofluid

Chapter 1

Introduction and literature review

1.1 Introduction

Conventional heat transfer liquids have weak thermal conductivity as compared to solids. Advanced miniaturized technologies with comparatively small channels would get blocked, if conventional fluids which contain mm or nm sized particles were to be used. Choi coined the term "nanofluids," which are engineered colloids consisting of a base fluid and nanoparticles. Nanofluids are one of the most recent advancements in nanotechnology. Nanofluids are high-efficiency heat-transfer fluids made by dispersing nanoparticles with diameters less than 100 nm in conventional fluids. Due to the occupancy of a significant number of atoms on boundaries, nanoparticles have a wider surface area to volume ratio than microparticles, providing them with high thermal stability in suspensions. Nanofluids have enhanced properties such as thermal conduction. The properties like enhanced stability and better conductivity of the scattered Nano-species make them highly desirable for developing heat transit fluids. As various industrial products such as power electronic circuits, high power lasers, x-ray generators *etc.* require cooling for better performance.

As an extension of nanofluid, hybrid nanofluid is developed by dispersing composite two distinct nanoparticles in the base fluid. As a consequence, it is expected that hybrid

nanofluid would have better thermal conductivity than base fluid and nanofluid containing single nanoparticles. In recent years, researches have focused on developing hybrid nanofluids that should be more stable and sustainable, with reduced viscosity and high thermal conduction. These fluids have transformed a wide range of heat transfer functions, including cooling, nuclear systems, solar heating, drug reduction, biomedical etc. As a result, these industrial applications require stable and unique production techniques for hybrid nanofluids using less expensive equipment.

Stratification is a major aspect of heat and mass transmission that is being studied by a number of scientists.It occurs in flow fields due to temperature changes, concentration differences, or varying liquid densities. Because of its vast range of natural, industrial, and engineering uses, it is important to expose the impact of stratification on the mechanism of convective transport in real-world applications. Thermal stratification of reservoirs and seas, heterogeneous mixtures in the atmosphere, industrial food and manufacturing processes, and the salinity stratification phenomenon in rivers, ground water reservoirs, and oceans are examples of these applications.Thermal stratification has the disadvantage of preventing oxygen from mixing from the upper to lower layers of water, causing water to become anoxic as a result of biological activity.

Magnetohydrodynamics is the analysis of the magnetic characteristics and behaviour of electrically conducting fluids. Plasmas, liquid metals, salt water, and electrolytes are some examples of magnetofluids. Many manufacturing processes, such as drawing of copper wires, continuous stretching of plastic films and artificial fibres, glass-fiber, metal extrusion, and spinning, depend on investigations of magnetohydrodynamic (MHD) boundary layer flow and heat transfer of viscous fluids over a flat sheet. The magnetohydrodynamic (MHD) concept is used to generate electricity from coal-fired or nuclear power plants. MHD generating plants do not require a turbine and do not have a generator shaft. Thermal energy in plasma is converted directly to electrical energy in an MHD generator. When an electric conductor passes through a magnetic field, it generates a voltage, which results in an electric current. The solid conductors in an MHD generator

are replaced with a gaseous conductor, an iodized gas.When such a gas is moved at high speed through a strong magnetic field, a current is generated that can be collected by placing electrodes in appropriate positions in the stream.

Fourier's coined work was regarded as the most appropriate method that has been used as a guideline for decades because of its wide-ranging applications. One of the model's flaws is that it frequently leads to a parabolic energy equation indicating that the initial disturbance was immediately observed by the medium under consideration. Cattaneo introduced relaxation time to address a flaw in Fourier's law known as the "Paradox in heat conduction". It can be seen that this modification results in the hyperbolic energy equation and allows heat to be transported via propagation of thermal waves with limited speed. Christov later improved Cattaneo's model by substituting the time derivative for the upper convected derivative of the Oldroyd equation. This improved version is now known as the Cattaneo-Christov heat flux model.

1.2 Literature Review

The advancements in the field of nanofluids have the potential to be significant due to its wide usage in daily life and advanced heat and mass transport processes such as domestic refrigerators, hybrid-powered engines, heat exchangers, solar water heating, nuclear reactors, chillers, and pharmaceutical processes, [1-2]. Choi and Eastman [3-5] coined the term "nanofluids." These fluids are created by dispersing nanoparticles in traditional fluids to increase thermal conductivity. A nanofluid is a new type of heat transfer fluid that consists of a base fluid mixed with nanoparticles. It has been demonstrated that nanofluids increase the thermal conductivity and convective heat transfer performance of base liquids. Brownian movements of nanoparticles inside the base fluids are one of the proposed causes for the unusual increase in thermal conductivity of nanofluids. Tiwari and Das [6] proposed a two-stage model for analysing nanofluids that combined powerful thickness, consistency, warm, and electrical conductivities. It should be noted

that several recent papers [7-8] have been published on the mathematical and numerical modelling of natural convection heat transfer in nanofluids. Buongiorno [9], Kakac and Pramuanjaroenkij [10], conducted an extensive study of convective transport in nanofluids. Khan and Pop [11] investigated the boundary layer flow of a nanofluid past a stretching sheet using the Buongiorno model. Rana and Bhargava [12] studied the boundary layer flow of a nanofluid flow over a non-linearly stretching sheet recently. Many researchers were intrigued by the boundary layer flow of a nanofluid induced by a stretching surface [13-15].

Turcu et al. [16] and Jana et al. [17] proposed the concept of "hybrid nanofluid" in their experimental works to improve the thermal properties of regular nanofluid. A hybrid nanofluid is a liquid that has been developed and consists of more than one nanoparticle with synergistic and improved heat transfer properties immersed in a conventional fluid [18-19]. The concept of hybrid nanofluids with enhanced heat transfer characteristics in comparison to ordinary nanofluids has piqued the interest of researchers who want to explore new avenues for increased heat transfer rates. Rostami et al. [20] use a two-step technique to conduct an experimental hybrid nanofluid synthesis study with graphene oxide, copper oxide nanoparticles combined with water, and ethylene glycol at temperatures ranging from $25°to50°C$. The study reveals that with a volume fraction of less than 0.4 percent, the nanofluid exhibits Newtonian behaviour, but as the concentration increases above 0.4%, the nanofluid viscosity is affected by an increase in shear rate. Taherialekouhi et al. [21] investigated the thermal conductivity of a hybrid nanofluid containing graphene oxide and aluminium oxide nanostructures immersed in water with volume fractions of $0.1, 0.25, 0.5, 0.75$, and 1%at temperatures ranging from 25 to $50°C$ in another experiment. When the volume fraction is considered as 1% at $50°C$, the results show an increase in thermal conductivity of up to 33.9%. Kaska et al. [22] investigated the heat transfer properties of a hybrid nanofluid $(AlN - Al_2O_3/H_2O)$ inside an elliptical tube with varying nanoparticle volume concentrations. Mdallal et al. [23] investigated the flow of various types of hybrid nanofluids over a flat plate with Marangoni bound-

ary conditions while subjected to radiation and an inclined magnetic field. Waini et al. [24] studied the heat transfer phenomenon of a hybrid nanofluid flowing over a stretchable sheet and discovered that a higher nanoparticle concentration results in more heat transfer. The effects of a magnetic field and suction on a moving plate covered with a water-based hybrid nanofluid were investigated by Aladdin et al. [25]. Furthermore, the effects of suction and MHD on velocity and thermal field have also been discussed. Some important research in the field of nanofluid dynamics are present in [26-32].

The research of MHD flows, the Hall current, and ion slip relations in Ohms law have been ignored in order to easily conduct scientific examination of the flow. Nonetheless, the effect of the Hall current and ion slip is considerable in the presence of a strong magnetic field. Thus, it is critical to include the influence of Hall current and ion slip terms of the magnetohydrodynamics articulations under a variety of typical circumstances. As a result of these facts, various research have been conducted on MHD flows in the presence of Hall and ion slip currents. Accordingly, Gul et al. [33] scrutinize the effects of hall and ion slip in a thermally stratified nanofluid flow comprising Cu and Al_2O_3 nanoparticles on a nonlinear stretchable sheet with the effect of nonuniform heat source sink. It is discovered that as the magnetic field intensity is increased, the temperature of the nanofluid increases. The rise in Ohmic and viscous dissipations causes this enchantment in the temperature of the liquid. Using a Maxwell liquid over an extending vertical surface, Nawaz et al. [34] investigated the Hall and ion slip impacts on three-dimensional combined free and forced convection flow of a Maxwell liquid. They found that the Hall parameter has similar impacts on both the tangential and the lateral velocities, whereas the ion slip parameter has opposite impacts on both the velocities. The effects of Hall and ion slip on the three-dimensional flow equations of nano-plasma fluid in the presence of a homogeneous applied magnetic field were also investigated by Nawaz and Zubair [35], who discovered that the inclusion of copper (Cu) and silver (Ag) nanoparticles has a significant impact on the velocity components and temperature of the nano-plasma. Ramzan et al. [36] examined the dynamics of Hall effect and Ion slip effects on the flow

of natural fluids over the birectional stretching sheet are altogether distinct in comparison to the flow of natural. There are also further research articles incorporating the effects of Hall and ion slip currents in the references [37–40].

The current study is inspired by previous studies and seeks to examine the effects of Hall current and Ion slip on a hybrid nanofluid flow with a non-uniform source/sink. Such a study, to the best of knowledge, has not yet been done. All results presented in graphs and tables are thoroughly examined.

Chapter 2

Preliminaries

2.1 Fluid

A material that deforms continuously under forced shear stress or external pressure is fluid. Fluids are a substance form of liquids , gases, and plasma.

2.2 Nanofluid And Base fluid

A nanofluid is a fluid in which nanometer-sized particles suspended in a base fluid form a colloidal solution of nanoparticles. The nanoparticles used in nanofluids are often formed of metals, oxides, carbides, or carbon nanotubes, with water, ethylene glycol, and oil serving as the base fluids. Nanoparticles are employed to improve the fluid's thermal conductivity.

2.3 Hybrid Nanofluid Flow

The thermal properties of the nanofluid might be improved by adding more than one nanoparticle into the basic fluid, which was termed "hybrid nanofluid." A hybrid nanofluid is an advanced fluid that contains more than one nanoparticle capable of increasing the

heat transfer rate.

2.4 Fluid mechanics

The branch of mechanics concerned with fluid characteristics. It is divided into two subcategories, which are as follows:

2.4.1 Fluid statics

It is the sub branch which investigates the attributes of liquids in stationary state.

2.4.2 Fluid dynamics

It is the sub branch which investigates the attributes of liquids in state of motion.

2.5 Stress

Stress is defined as the ratio of applied force F to cross section area A. Symbolically, we have

$$Stress = \frac{F}{A}. \tag{2.1}$$

In the SI system the unit of stress is kg/m.s^2 and the dimension is [(M/(LT^2))]. It is further categorized into 2 kinds.

2.5.1 Shear stress

Shear stress is the kind of stress when external force acts parallel to the unit area of the surface.

2.5.2 Normal stress

Normal stress is the kind of stress when force acts vertical to the surface of unit area.

2.6 Strain

Strain is the dimensionless quantity, which is used to measure the deformation of an object when a force is applied on it.

2.7 Flow

Flow is characterized as a material that deforms smoothly and fluently under the impacts of various kinds of forces. Flow is further divided into two major subclasses as follows:

2.7.1 Laminar flow

Laminar flow is obtain when the fluid travels in regular paths, with no interruption between the layers.

2.7.2 Turbulent flow

Turbulent flow is obtain when the fluid particles have irregular velocity in the flow field.

2.8 Viscosity

Viscosity is fundamental property of fluid that measures the fluid's resistance to flow when numerous forces are acting on it. Mathematically can be represented as follows

$$viscosity = \frac{shearstress}{\text{grad}\, ient\ of\ velocity}. \tag{2.2}$$

2.8.1 Dynamic viscosity

Dynamic viscosity (μ) also called absolute viscosity is the maesure of internal resistance to flow. Its dimension is $ML^{-1}T^{-1}$and its unit is Kg/ms.

2.8.2 Kinematic viscosity (ν)

Kinematic viscosity is defined as the ratio of absolute viscosity (μ) to the density of fluid (ρ) . Mathematically it is represented by

$$\nu = \frac{\mu}{\rho}. \tag{2.3}$$

Its SI unit is m^2/s and its dimension is $[((L^2)/T)]$.

2.9 Newton's law of viscosity

It is stated that the shear stress is directly proportional to the velocity gradient. Mathematically, it can be expressed as follows:

$$\tau_{yx} \propto \frac{du}{dy}, \tag{2.4}$$

or

$$\tau_{yx} = \mu \frac{du}{dy}, \tag{2.5}$$

in which τ_{yx} indicate the shear force applied on the fluid's element and μ indicate the proportionality constant.

2.9.1 Newtonian fluids

These are the fluids which satisfy the Newton's law of viscosity and fluid with a constant viscosity. In these fluids shear force τ_{yx} is proportional linearly to the gradient of velocity

$\frac{du}{dy}$. Alcohol, water, glycerine and kerosene are common examples of Newtonian fluids.

2.9.2 Non-Newtonian fluids

These are the type of fluids which donot satisfy the Newton's law of viscosity. Here, nonlinear and direct relationship exists between shear stress τ_{yx} and gradient of velocity. Mathematically, it is expressed as:

$$\tau_{yx} \propto (\frac{du}{dy})^n \qquad n \neq 1, \tag{2.6}$$

or

$$\tau_{yx} = \eta \frac{du}{dy} \quad , \quad \eta = m(\frac{du}{dy})^{n-1}, \tag{2.7}$$

where η the apparent viscosity, n the flow behaviour index and m the consistency index. For n=1 above eq. converts to Newton's law of viscosity. Yougurt, fabric, paints and ketchup exhibits the non-Newtonian fluid behavior. These fluids are classified mainly into three- kinds such as differential type, integral type and rate type. The fluid models which are considered in this dissertation are subclass of a differential type fluid namely second order fluid and second grade fluid. Stress tensor presented by Cauchy for the first order and second order fluids are expressed as

$$\tau = -pI + \mu A_1, \qquad \tau = -pI + \mu A_1 + \alpha_1 A_2 + \alpha_2 {A_1}^2, \tag{2.8}$$

whereA_1 and A_2 denote the first and second Rivlin-Ericksen tensors, $i.e$,

$$A_1 = (\nabla.V) + (\nabla.V)^T, \tag{2.9}$$

$$A_2 = \frac{dA_1}{dt} + A_1(\nabla.V) + (\nabla.V)^T A_1. \tag{2.10}$$

2.10 Density

Mass of a material per unit volume is known as density. This quantity is used to measure the amount of matter that is present in a certain volume of it.

Mathematically expessed as follows:

$$\rho = \frac{\mu}{\upsilon}. \tag{2.11}$$

The SI unit of density is kg/m^3.

2.11 Pressure

Pressure is defined as force exerted on a surface per unit area.

Mathematically expressed the pressure is given by:

$$P = \frac{F}{A}. \tag{2.12}$$

N/m^2 is the SI unit of pressure..

2.12 Mechanism of heat transfer

Heat is a form of energy which transmits from warmer to colder region. Heat transfer phenomenon arises between two objects which are placed at different temperatures. The dispersion of heat takes place by means of three main mechanism, conduction, convection and radiation.

2.12.1 Conduction

Conduction is a procedure in which heat transfer from hot area to the cool area of liquids and solids by collisions of free electrons and molecules. In this phenomenon molecules are not transferred. Mathematically,

$$\frac{q}{A} = K\frac{T_1 - T_2}{X_1 - X_2} = K\frac{\triangle T}{\triangle X}, \tag{2.13}$$

or

$$q = -kA\frac{dT}{dx}, \tag{2.14}$$

in which q represents the heat flow, A the area of the surface, k the thermal conductivity, T_1 temperature is greater than T_2 , (dT)/(dx) denotes the temperature gradient and heat is conducted from high to low temperature when the sign is negative.

2.12.2 Convection

In this process heat transfer from hot to region of liquids and gases due to the motion of molecules. Mthematically,

$$q = hA[T_S - T_\infty], \tag{2.15}$$

here h is for convective heat transfer coefficient, T_S for system temperature, A for the area and T_∞ for the reference temperature.

2.12.3 Radiation

A process in which the heat is transferred by the electromagetic waves is called radiation. This process plays vital role when heat is transferred through vacuum. Mthematically,

$$q = e\sigma A(\triangle T)^4, \tag{2.16}$$

where q denotes the heat transfer, e for emissivity of the system, σ for the constant Stephen-Boltzmann, A for area and $(\triangle T)^4$ for the temperature difference between two systems fourth power.

2.13 Dimensionless numbers

2.13.1 Reynolds number

It is the most important dimensionless number which is utilized to recognize the distinctive flow behaviors like laminar and turbulent flow. It depicts the inertial to viscous forces ratio. Mathematically it can be expressed as:

$$Re = \frac{VL}{v}. \tag{2.17}$$

Here V denotes the velocity of fluid, L represents the characteristic length and v stands for kinematic viscosity. Reynolds number are used to characterize different flow regimes within a similar fluid, such as laminar or turbulent flow. At low Reynolds number laminar flow arise, where viscous forces are dominant. At high Reynolds number turbulent flow arise, where inertial forces are dominant.

2.13.2 Prandtl number

The ratio of Momentum diffusivity (v) to thermal diffusivity (α) is known as Prandtl number. Mathematically, it can be expressed by

$$Pr = \frac{\nu}{\alpha} = \frac{\mu C_p}{k}, \tag{2.18}$$

in which μ represents the dynamic viscosity, C_p denotes the specific heat and k stands for thermal conductivity. The Prandtl number is used in heat transfer to control the thicknesses of momentum and thermal boundary layers.

2.13.3 Skin friction coefficient

When fluid is passing across a surface certain amount of drag appears which is known as skin friction. It occurs between the fluid and the solid's surface which leads to slow down the motion of fluid. The skin friction coefficient can be defined as:

$$C_f = \frac{\tau_w}{1/2\rho U_w^2}. \tag{2.19}$$

in which τ_w stands for wall shear stress, ρ stands for density and U_w represents the velocity.

2.13.4 Nusselt number

The dimensionless quantity which represents the convective to conductive heat transfer ratio is known as Nusselt number. Mathematically,

$$Nu_L = [(h\triangle T)/(k\triangle T/L)] = ((hl)/k), \tag{2.20}$$

where h stands for convective heat transfer, L for characteristic length and k for thermal conductivity.

2.14 Fundamental laws

The fundamental laws that are used for the flow specification in the subsequential analysis are given below.

2.14.1 Law of mass conservation

It states that in any closed system, the total mass will remain constant. Mathematically

$$\frac{D\rho}{Dt} + \rho\nabla.V = 0, \tag{2.21}$$

or

$$\frac{\partial\rho}{\partial t} + (V.\nabla)\rho + \rho\nabla.V = 0, \tag{2.22}$$

or

$$\frac{\partial \rho}{\partial t} + (V.\nabla)\rho = 0. \tag{2.23}$$

It is known as the equation of continuity. For the steady flow above eq. becomes:

$$\nabla.(\rho V) = 0, \tag{2.24}$$

and if the fluid is incompressible then above Eq. implies that

$$\nabla.V = 0. \tag{2.25}$$

2.14.2 Law of momentum conservation

It is stated that the total linear momentum of a closed system is constant. Generally it is given by:

$$\rho \frac{DV}{Dt} = \text{div}\, \tau + \rho b, \tag{2.26}$$

where τ is Cauchy stress tensor and b is for body force.

2.14.3 Law of energy conservation

Law of conservation of energy is also known as energy equation and is given by:

$$\rho \frac{De}{Dt} = \tau.L - \nabla.q + \rho r, \tag{2.27}$$

in which e stands for specific internal energy, q for heat flux vector and r for thermal radiation. Energy equation without thermal radiation takes the form:

$$\rho C_p \frac{DT}{Dt} = \tau L + k\nabla^2 T, \tag{2.28}$$

where $e = C_p T$, $q = k\nabla T$, k denotes the thermal conductivity and T for temperature.

2.14.4 Law of conservation of concentration

For nanoparticles the volume fraction equation is:

$$\frac{\partial C}{\partial t} + V.\nabla C = -\frac{1}{\rho_p}\nabla.j_p, \tag{2.29}$$

$$\frac{\partial C}{\partial t} + V.\nabla C = D_B\nabla^2 C + D_T(\frac{\nabla^2 T}{T_\infty}). \tag{2.30}$$

2.14.5 Thermal diffusivity

Thermal diffusivity is a material specific property for describing the unsteady conductive heat flow. This value describes how speedily a material respond to change in temperature. It is ratio between thermal conductivity and the product of specific heat capacity and density. Mathematically,

$$\alpha = \frac{k}{\rho C_p}, \tag{2.31}$$

where thermal conductivity is represented by k., specific heat capacity is represented by C_p and density is represented by ρ.

2.14.6 Thermal conductivity

The ability of a material to conduct heat is determined by thermal conductivity. Acoording to Fourier Law of heat conduction ,it is described as " The amount of heat transfer rate (Q) through a material of unit thickness (L) times unit cross section area (A) and unit temperature difference ($\triangle$T)". Mathematically written as:

$$k = [(QL)/(A(\triangle T))]. \tag{2.32}$$

In SI system thermal conductivity unit is W/(m.K) and dimension is (ML)/($T^3\theta$).

2.15 Hall Effect

The Hall effect is the motion of charge carriers through a conductor in the direction of a magnetic attraction. The effect is named after Edwin Hall, who discovered it in 1879. The effect is magnified in a semiconductor due to the presence of moving positive charge carriers known as Halls.

$$F_m = eV_dB, \tag{2.33}$$

where V_d is the drift velocity of the charge.

Chapter 3

Comparative analysis of magnetized partially ionized Copper, Copper Oxide-water and kerosene oil nanofluid flow with Cattaneo-Christov heat flux

In this comparative study, the impact of two different nanoparticles, Copper and Copper Oxide, in two different partially ionized magneto nanofluid flows (water and kerosene oil mixed with Copper/Copper Oxide) over a linearly stretching surface is investigated. In the presence of the Cattaneo-Christov heat transfer model, the effects of electron and ion collisions are also investigated. The effects of key parameters on velocity and temperature fields are graphically represented. The nonlinear partial differential equations are transformed using a similarity transformation procedure. Our numerical methodology is based on the Finite difference method, which is the standard method in the MATLAB scheme's bvp4c built-in function. Our findings show that the effects of CuO on nanofluid velocity are greater than those of Cu. The temperature of the fluid is more noticeable

when the concentration of nanoparticles in Cu-water nanofluid is increased.

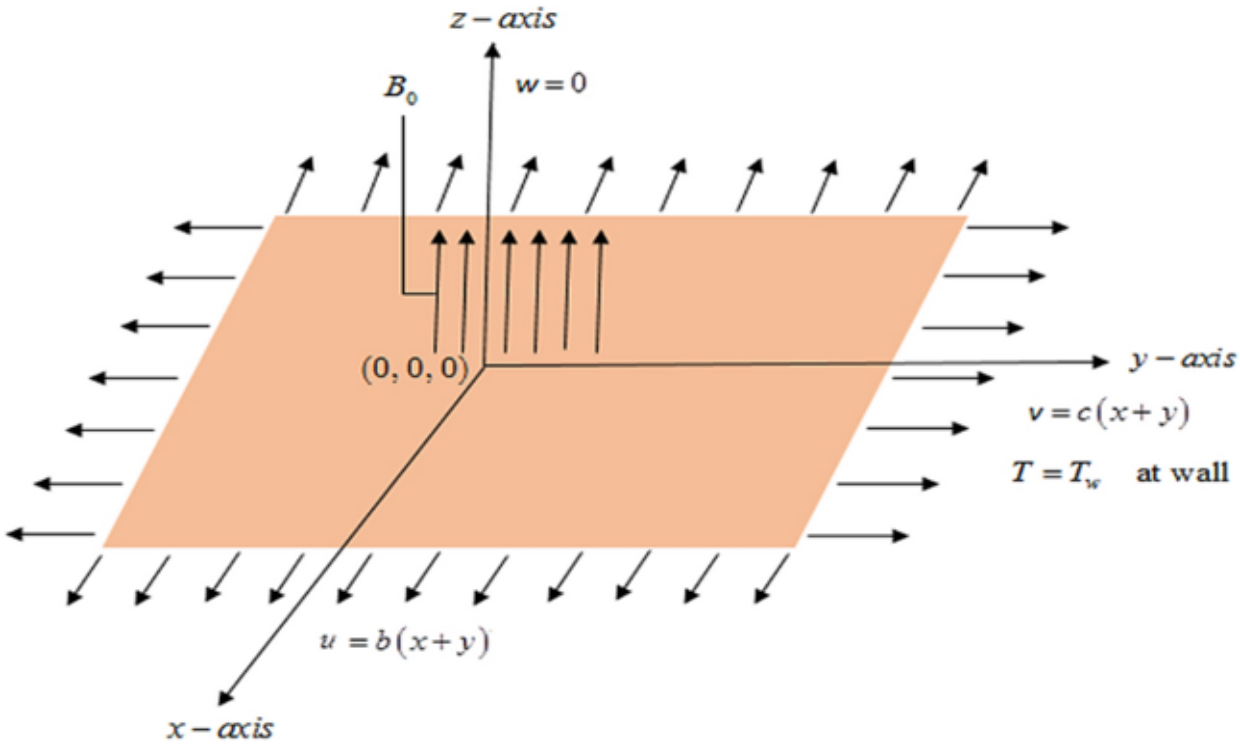

Fig. 3.1 Flow diagram of the mathematical model

3.1 Mathematical Formulation

Partially ionised magnetised nanofluid flows over a horizontal stretching sheet in a constant magnetic field, with (C-C) heat flux taken into account. The velocity of a magnetised partially ionised nanofluid is $V_w = [b(x + y), c(x + y), 0]$. The below are the magnetohydrodynamic (MHD) equations for the incompressible time-independent flow of Newtonian fluid with invariable properties.

$$U_x + V_y + W_z = 0, \tag{3.1}$$

$$UU_x + VU_y + WU_z = \upsilon_{nf} U_{zz} + \frac{\sigma_{nf}\beta_0^2[-V\beta_e + U(1+\beta i\beta_e)]}{\rho_{nf}\left[(1+\beta_e\beta i)^2 + (\beta_e)^2\right]}, \tag{3.2}$$

$$\begin{aligned} UV_x + VV_y + WV_z &= \upsilon_{nf} V_{zz} - \frac{\sigma_{nf}\beta_0^2[U\beta_e + V(1+\beta i\beta_e)]}{\rho_{nf}\left[(1+\beta_e\beta i)^2 + (\beta_e)^2\right]}, \qquad (3.3)\\ UT_x + VT_y + WT_z &= \frac{k_{nf}}{(\rho C_p)_{nf}} T_{zz} - \frac{\tau_o}{(\rho C_p)_{nf}}\{W^2 T_{zz} \\ &\quad + (UW_x + VW_y + WW_z)T_z\}. \qquad (3.4) \end{aligned}$$

The boundary conditions listed below are utilized to interpret the problem:

$$\begin{aligned} U|_{z=0} &= b(y+x),\ V|_{z=0} = c(y+x),\ W|_{z=0} = 0,\ T|_{z=0} = T_w,\\ U|_{z\to\infty} &= 0,\ T|_{z\to\infty} = T_\infty. \end{aligned}$$

The thermophysical properties are:

$$\begin{aligned} \mu_{nf} &= \mu_f(1-\varphi)^{-2.5},\\ \nu_{nf} &= \frac{\mu_{nf}}{\rho_{nf}},\\ \rho_{nf} &= (1-\varphi)\rho_f + \varphi\rho_n, \qquad (3.5)\\ (\rho C_p)_{nf} &= (1-\varphi)(\rho C_p)_f + \varphi(\rho C_p)_n,\\ \frac{k_{nf}}{k_f} &= \frac{(k_n+2k_f) - 2\varphi(k_f - k_n)}{(k_n+2k_f) + \varphi(k_f - k_n)},\\ \sigma_{nf} &= (1 + \frac{3(\frac{\sigma_n}{\sigma_f} - 1)\phi}{\frac{\sigma_n}{\sigma_f} + 2 - (\frac{\sigma_n}{\sigma_f} - 1)\varphi})\sigma_f. \end{aligned}$$

3.2 Similarity Transformation

Following transformation is used to convert PDE's to ODE's:

$$\begin{aligned} U &= b(x+y)F'(\eta),\ V = b(x+y)G'(\eta),\ W = -(bv_f)^{1/2}[F(\eta)+G(\eta)], \\ \eta &= (b/v_f)^{1/2}z,\ T = (T_w - T_\infty)\theta(\eta) + T_\infty. \end{aligned} \tag{3.6}$$

Making use of similarity transformations equation of continuity is identically satisfied and the ordinary non-dimensional system of equations along with boundary conditions take the following form:

$$(\frac{1}{\varphi_1})F''' + F''(F+G) = F'(F'+G') + (Ha)^2(\frac{\varphi_2}{\varphi_1})[\frac{(1+\beta e\beta_i)F' - \beta_e G'}{(1+\beta_e\beta_i)^2+\beta_e^2}], \tag{3.7}$$

$$(\frac{1}{\varphi_1})G''' + G''(F+G) = G'(F'+G') + (Ha)^2(\frac{\varphi_2}{\varphi_1})[\frac{(1+\beta e\beta_i)G' - \beta_e F'}{(1+\beta_e\beta_i)^2+\beta_e^2}], \tag{3.8}$$

$$(\frac{1}{\varphi_3}\frac{K_{nf}}{K_f})\theta'' = \Pr[\gamma\{(F+G)^2\theta'' + (F+G)(F'+G')\theta' - (F+G)\theta'\}], \tag{3.9}$$

with boundary conditions

$$\begin{aligned} F(0) &= 0, G(0) = 0,\ F'(0) = 1, G'(0) = a,\ \theta(0) = 1, \\ F'(\infty) &\to 0,\ G'(\infty) \to 0,\ \theta(\infty) \to 0, \end{aligned}$$

where

$$\begin{aligned}
\phi_1 &= (1-\phi)^{2.5}(1+\phi-\phi\frac{\rho_n}{\rho_f}),\\
\phi_2 &= (1-\phi)^{2.5}\{1+\frac{3(\frac{\sigma_n}{\sigma_f}-1)\phi}{\frac{\sigma_n}{\sigma_f}+2-(\frac{\sigma_n}{\sigma_f}-1)\phi}\},\\
\phi_3 &= (1+\phi-\phi\frac{(\rho C_p)_n}{(\rho C_p)_f}).
\end{aligned} \tag{3.10}$$

The expression for the non-dimensional parameter given in equation (3.8)-(3.11) are:

$$a=\frac{c}{b},\ Ha=(\frac{\sigma_{nf}B_o^2}{b\rho_f})^{\frac{1}{2}},\ \ \mathrm{Pr}=\frac{\mu_f(C_p)_f}{k_f},\ \gamma=\tau_o b. \tag{3.11}$$

Dimensional form of Surface drag co-efficient and Nusselt number are;

$$\begin{aligned}
C_x &= \frac{\tau_{zx}}{\rho_f u^2}, C_y=\frac{\tau_{zy}}{\rho_f v^2}, Nu_x=\frac{(x+y)q_w}{k_f(T_w-T_\infty)},\\
\tau_{zx} &= \mu_{nf}(u_z+w_x),\ \tau_{zy}=\mu_{nf}(u_z+w_y),
\end{aligned} \tag{3.12}$$

with equation (3.7), we obtain a non-dimensional form of surface drag co-efficient and Nusselt number given as follows:

$$\begin{aligned}
(\mathrm{Re}_{x_L})^{0.5}C_x &= \frac{1}{\varphi_1}F'(0),\\
(\mathrm{Re}_{y_L})^{0.5}C_y &= \frac{1}{\varphi_1}G'(0),\\
(\mathrm{Re}_{x_L})^{0.5}Nu_x &= -\frac{k_{nf}}{k_f}\theta'(0),
\end{aligned} \tag{3.13}$$

Re_{x_L} and Re_{y_L} are local Reynolds number, which are expressed as:

$$Re_{x_L}=\frac{b(x+y)}{\nu_f}, Re_{y_L}=\frac{c(x+y)}{\nu_f}. \tag{3.14}$$

3.3 Results and Discussion:

In the presence of the C-C heat flux model, the heat transfer impacts of Cu and CuO nanoparticles in partially ionised magnetic nanofluids based on water and kerosene oil are theoretically investigated. The numerical default approach of the bvp4c built-in function is used to solve the mathematical system of equations. The different effects are numerically modelled and displayed in both graphical and table formats. Fluid flow, shears and heat transfer rates on the wall, is examined under a number of physical conditions in both x and y directions. The variables used in analysis are β_e, β_i, a, γ. Figures 3.2 and 3.3 depict the impacts of (a= c/b) on the x and y velocity profile, which are the ratio of the rate of stretched surface c in the y-direction to the rate of stretched surface c in the x-direction. The momentum diffusion of y-direction is slower than x-direction. The velocity of partly ionised nanofluid flow is larger in the case of CuO-kerosene oil nanofluid, to the extent that the velocity of CuO-kerosene oil nanofluid surpasses the rate at which b is stretched in the x-axis. As a result, it may be deduced that velocity increases in the y direction and decreases in the x direction. Figs. 3.4 and 3.5 shows that the x component of velocity increases as (β_e) increases, while the y component of velocity decreases. Figures 3.6 and 3.7 depict the impact of β_i on the x and y axes. As the Ion slip factor is raised, the fluid velocity increases in both the x and y axes. It depicts that behavior of β_i on x -compoenets is same as β_e on x components of partially ionized fluid. As the fluid speed increases due to ion collisions τ_i in time or the frequency of ions (ω_i) increases as a result of an increase in the ion slip parameter, velocity rises. The decreasing trend of the stretching ratio parameter with relation to fluid temperature is seen in Figure 3.8. Temperature variations in Cu-water nanofluids are greater than in CuO-kerosene oil nanofluids. Fig. 3.9 depicts the observations for partially ionised fluid temperature as a function of the thermal time relaxation parameter. The temperature of a partially ionised nanofluid is lowered as the value of γ decreases. Furthermore, the zero thermal relaxation time is consistent with existing methods. According to Fourier's law, the temperature is lower than the conventional Fourier's model. Cu nanoparticles

distributed in partially ionised water-base fluid have the greatest temperature than the other three partially ionised water-base fluids under the impact of prominent factors nanofluids that have been ionised.

Tables 3.1(a,b),3.2(a,b), and 3.3(a,b) demonstrate the impact of various variables on heat transfer and skin drag . The table illustrates numeric values for heat flux and skin drag for two types of partially ionized fluids (water and kerosene oil) versus two types of nanoparticles volume fraction φ, Hartmann number Ha, thermal time relaxation parameter γ, Hall and ion slip parameters β_e and βi, and stretching ratio parameter a for two types of partially ionised fluids (water and kerosene oil). When the Hall parameter β_e is raised, shear stress at the wall in the x-direction decreases, whereas shear stress at the wall increases when the ion slip parameter is increased. Shear stress at the y-direction wall decreases as the Hall parameter β_e grows, but shear stress at the y-direction wall increases when the ion slip parameter increases. When βi is increased, the heat flow at the wall increases. Numerical studies show that raising the thermal time relaxation parameter causes a modest increase in wall heat flux. As nanoparticle dispersion increases, so does

skin friction (both in the x and y axis) and flow of heat at the wall.

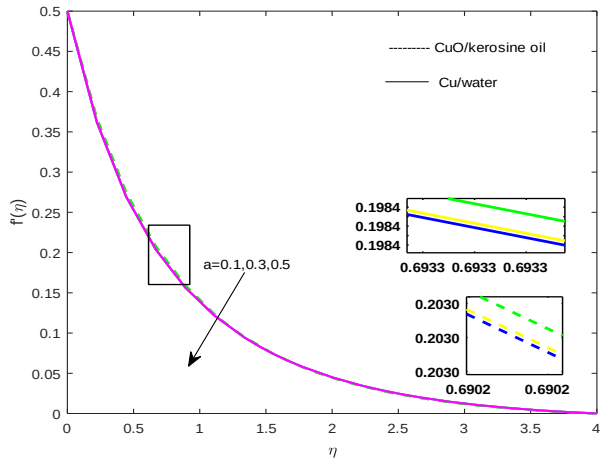

Fig. 3.2 Change in f′(η) vs a

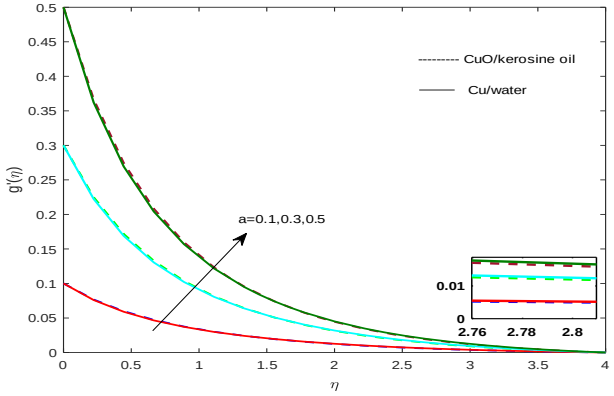

Fig. 3.3 Change in g′(η) vs a

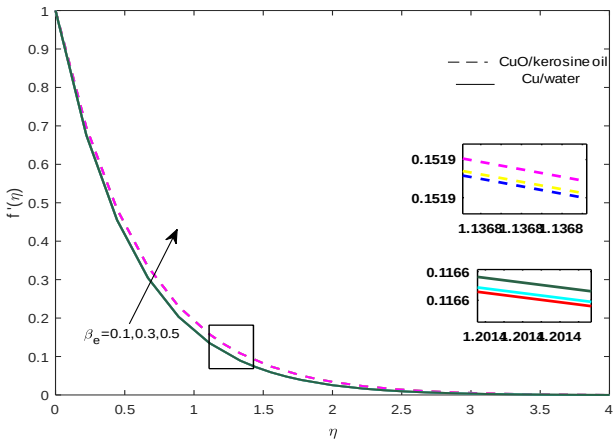

Fig. 3.4 Change in f′(η) vs β_e

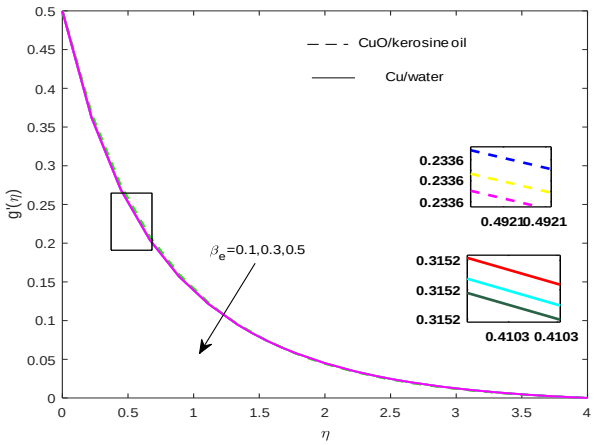

Fig. 3.5 Change in $g'(\eta)$ vs β_e

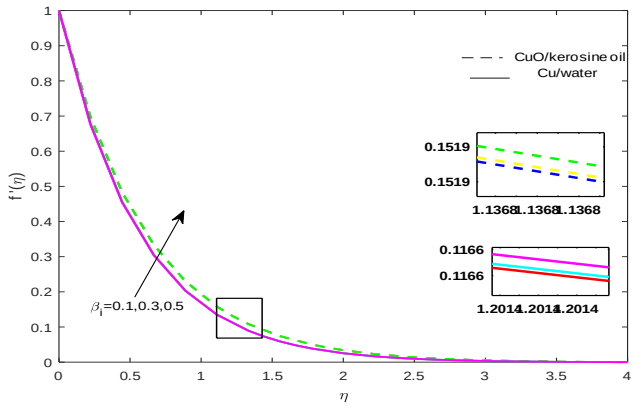

Fig. 3.6 Change in $\mathrm{f}'(\eta)$ vs β_i

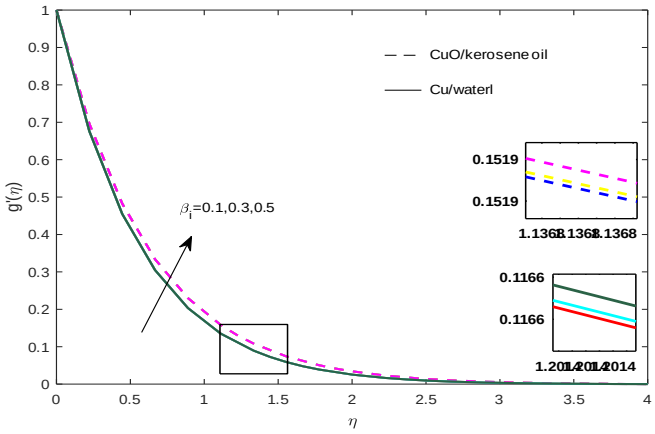

Fig. 3.7 Change in $\mathrm{g}'(\eta)$ vs β_i

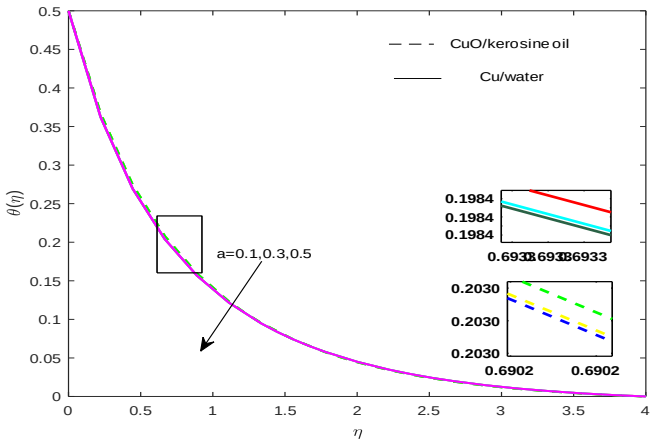

Fig. 3.8 Change in $\theta(\eta)$ vs a

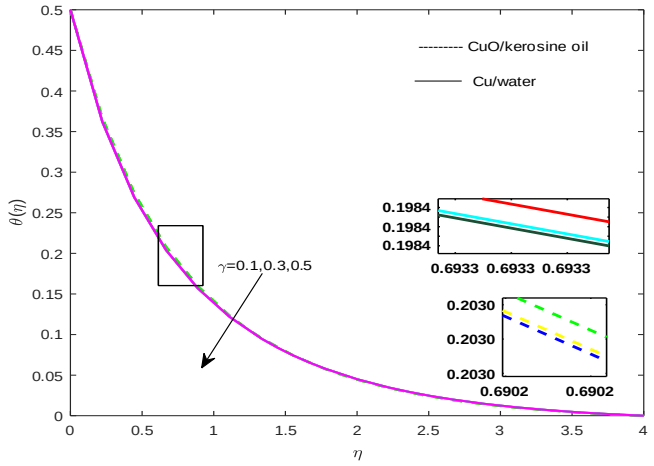

Fig. 3.9 Change in $\theta(\eta)$ vs γ

Table 3.1(a) Analysis of Skin/Surface drag in x-axis

φ_1	Ha	γ	β_e	β_i	a	Copper(water)	Copper Oxide(water)
0.01						-1.3478952	-1.3612856
0.02						-1.2809354	-1.3045165
0.03						-1.2209122	-1.2522615
0.01	0.1					-1.1690065	-1.1815156
	0.3					-1.1931705	-1.2065709
	0.5					-1.2399456	-1.2528109
	0.8	0.1				-1.3478952	-1.3612856
		0.3				-1.3478952	-1.3612856
		0.5				-1.3478952	-1.3612856
		0.5	0.1			-1.3652991	-1.3787380
			0.3			-1.3659952	-1.3612856
			0.5			-1.3670789	-1.3609839
			0.5	0.1		-1.3602233	-1.3736169
				0.3		-1.3537355	-1.3671276
				0.5		-1.3478952	-1.3612856
				0.5	0.1	-1.2289698	-1.2405280
					0.3	-1.2899924	-1.3024977
					0.5	-1.3478952	-1.3612856

Table 3.1(b) Analysis of Skin/Surface drag in x-axis

φ_1	Ha	γ	β_e	β_i	a	Copper(oil)	Copper Oxide(oil)
0.01						-1.3290680	-1.3468623
0.02						-1.2483745	-1.279019
0.03						-1.1782113	-1.2180605
0.01	0.1					-1.1558839	-1.1716080
	0.3					-1.1792828	-1.1960799
	0.5					-1.2240452	-1.2411975
	0.8	0.1				-1.3290680	-1.3471201
		0.3				-1.3290680	-1.3471201
		0.5				-1.3290680	-1.3471201
		0.5	0.1			-1.3460022	-1.3639729
			0.3			-1.3290680	-1.3468623
			0.5			-1.3264790	-1.3443249
			0.5	0.1		-1.3410002	-1.3589029
				0.3		-1.3347209	-1.3525666
				0.5		-1.3290680	-1.3468623
				0.5	0.1	-1.2105855	-1.2267139
					0.3	-1.2713945	-1.2885132
					0.5	-1.3290680	-1.3468623

Table 3.2(a) Analysis of Skin/Surface drag in y-axis

φ_1	Ha	γ	β_e	β_i	a	Copper(water)	Copper Oxide (water)
0.01						-0.7481555	-0.7549908
0.02						-0.7090244	-0.7208294
0.03						-0.6741528	-0.6895493
0.01	0.1					-0.5861337	-0.5923779
	0.3					-0.6094333	-0.6161330
	0.5					-0.6529924	-0.6596934
	0.8	0.1				-0.7481555	-0.7549908
		0.3				-0.7481555	-0.7549908
		0.5				-0.7481555	-0.7549908
		0.5	0.1			-0.7094796	-0.7162494
			0.3			-0.7481555	-0.7549908
			0.5			-0.8043621	-0.8113016
			0.3	0.1		-0.7690649	-0.7759392
				0.3		-0.7578884	-0.7647415
				0.5		-0.7481555	-0.7549908
				0.5	0.1	-0.1887964	-0.1900994
					0.3	-0.4546673	-0.4585576
					0.5	-0.7481554	-0.7549908

Table 3.2(b) Analysis of Skin/Surface drag in y-axis

φ_1	Ha	γ	β_e	β_i	a	Copper(oil)	Copper Oxide(oil)
0.01						-0.7366010	-0.7462150
0.02						-0.6891233	-0.7053459
0.03						-0.6481502	-0.6688613
0.01	0.1					-0.5795261	-0.5873872
	0.3					-0.6020764	-0.6105802
	0.5					-0.6442662	-0.6531216
	0.8	0.1				-0.7366010	-0.7463125
		0.3				-0.7366010	-0.7463125
		0.5				-0.7366010	-0.7463125
		0.5	0.1			-0.6990055	-0.7083001
			0.3			-0.7366010	-0.7462150
			0.5			-0.7911882	-0.8013409
			0.3	0.1		-0.7569085	-0.7667223
				0.3		-0.7460530	0.7557598
				0.5		-0.7366010	-0.7462150
				0.5	0.1	-0.1851113	-0.1873405
					0.3	-0.4471607	-0.4529255
					0.5	-0.7366010	-0.7462150

Table 3.3(a) Rate of heat transfer analysis

φ_1	Ha	γ	β_e	β_i	a	Copper(water)	Copper Oxide(water)
0.01						7.62570480	6.74610810
0.02						7.40457490	6.56191800
0.03						7.20182010	6.38516550
0.01	0.1					8.84073250	8.09590100
	0.3					8.56542160	7.80225640
	0.5					8.24273840	7.44828030
	0.8	0.1				7.62423740	6.68397270
		0.3				7.62497060	6.71482800
		0.5				7.62570480	6.74610810
		0.5	0.1			7.69683580	6.82813970
			0.3			7.62570480	6.74610810
			0.5			7.43556690	6.52417060
			0.3	0.1		7.53355578	6.63861360
				0.3		7.58225670	6.69550880
				0.5	0.1	7.62570480	6.74610810
					0.3	6.51155540	5.34888110

Table 3.3(b) Rate of heat transfer analysis

φ_1	Ha	γ	β_e	β_i	a	Copper(oil)	Copper Oxide(oil)
0.01						7.39028910	6.77532020
0.02						7.19080400	6.64042350
0.03						7.01120300	6.51230990
0.01	0.1					8.64775540	8.09759640
	0.3					8.35315670	7.81075800
	0.5					8.02400550	7.46420840
	0.8	0.1				7.38823010	6.70226120
		0.3				7.38925900	6.73769510
		0.5				7.39028910	6.77532020
		0.5	0.1			7.46333790	6.85591820
			0.3			7.39028910	6.77532020
			0.5			7.19450440	6.55655470
			0.3	0.1		7.29534810	6.66929950
				0.3		7.34553490	6.72542900
				0.5	0.1	7.39028920	6.77532020
					0.3	6.22776550	5.37534120

Chapter 4

Impact of Hall Current and Ion slip on a hybrid nanofluid flow with non-uniform source/sink

The flow of partially ionised magnetised 3D ZnO/Au-water and ZnO/Au-kerosene oil nanofluids over a linear stretching sheet with a constant magnetic field B_o as well as C-C heat flux is considered. Magnetized partially ionised nanofluid is moving at high speed. T_w is the surface temperature and T_∞ is the surrounding temperature. The effects of viscous and ohmic dissipation are not considered. There is no applied electric field because current charges are in motion. We neglected the induced magnetic field since high-velocity flow predicts a very low Reynolds number. The tables below exhibit the thermophysical properties of the associated base fluids, namely water and kerosene oil, as well as the nanoparticles, namely ZnO and Au.

4.1 Mathematical formulation

The assumptions of the envisioned mathematical model are given as under:

i. Three-dimensional partially ionized hybrid nanofluid flow over a linear extended

surface.

ii. The hybrid nanofluid flow is comprised of Zinc oxide, Gold, submerged into the kerosine oil and water.

iii.The impacts of the nonuniform source/sink are considered.

iv.The stretching velocity is taken as V=[b(x+y), c(x+y) , 0].

v. The wall and the ambient temperatures are taken as T_o and T_∞ respectively.

vi.The magnetic field B_o is taken along the z-axis.

vii.The induced magnetic field is ignored owing to the Reynolds number small values.

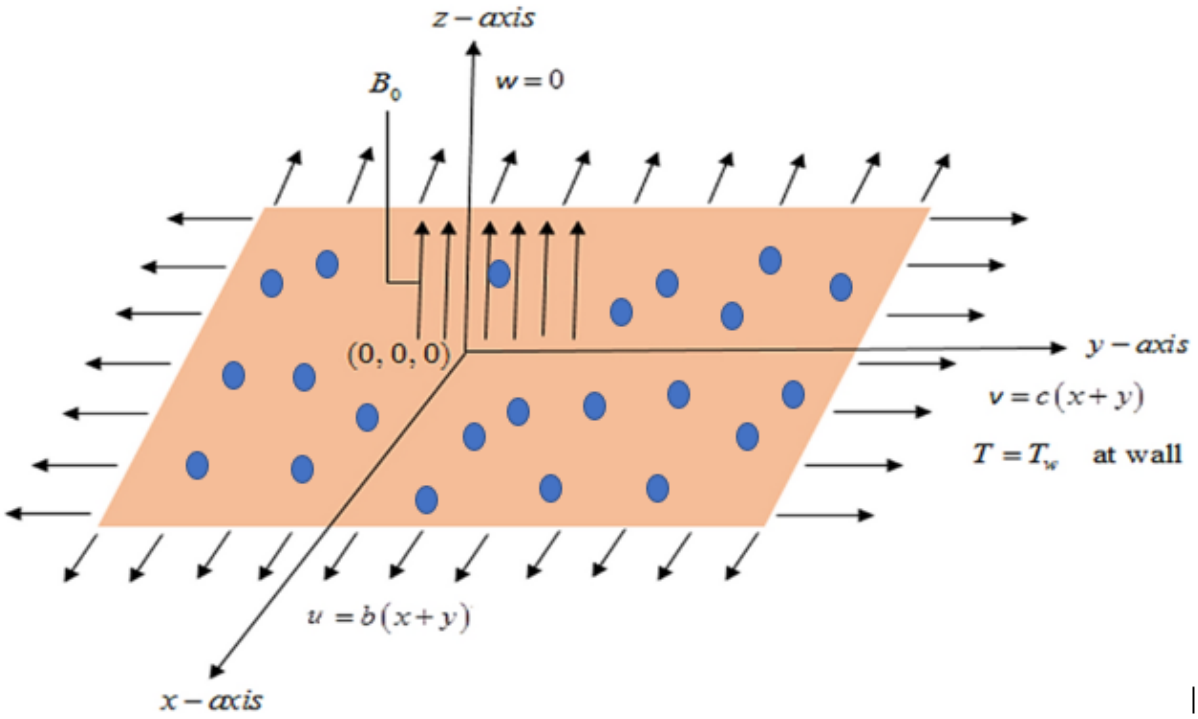

Fig. 4.1 Flow diagram of the mathematical model

MHD (Magnetohydrodynamic) equations for the steady, incompressible time-independent flow of Newtonian fluid with invariable properties are provided.

$$\bigtriangledown.\mathbf{V} = 0, \tag{4.1}$$

$$\rho_{hnf}.\frac{\mathbf{dV}}{\mathbf{dt}} = -\nabla\mathbf{P} + \rho_{hnf}^{-}(\mathbf{J}\times\mathbf{B}_0) + \ \mu_{hnf}\nabla^2\mathbf{V}, \tag{4.2}$$

$$\mathbf{J} = \sigma_{hnf}[\frac{\beta_e\beta_i}{|\mathbf{B}_\circ|^2}(\mathbf{J}\times\mathbf{B}_\circ)\times\mathbf{B}_\circ - \frac{\beta_e}{|B_\circ|}(\mathbf{J}\times B_\circ) + (\mathbf{E}+\mathbf{V}\times\mathbf{B}_\circ), \tag{4.3}$$

with C-C heat flux model

$$\mathbf{q} + \tau_o\{\mathbf{q}' + (\bigtriangledown.\mathbf{V})q + (\mathbf{V}.\bigtriangledown q) - q.\bigtriangledown\mathbf{V}\} = -k_{hnf}\bigtriangledown\mathbf{T}, \tag{4.4}$$

$$(\rho C_p)_{hnf}\mathbf{T}' + \tau_o\{\mathbf{V}.\bigtriangledown(\mathbf{V}.\bigtriangledown T)\} = k_{hnf}\nabla^2\mathbf{T} + \frac{1}{\sigma_{hnf}}\mathbf{J} + \mathbf{Q}. \tag{4.5}$$

Table 4.1 shows the thermophysical characteristics of the basic fluids used, namely water and kerosene oil, as well as the nanoparticles, namely ZnO and Au.

Table 4.1: Thermal properties of ZnO, Au, water and kerosineoil

Thermophysical Properties	ρ	C_p	k	σ
ZnO	5600	495.5	13	0.015
Au	19282	129	310	4.10×10^{7}
Water	997.1	4179	0.13	5.5×10^{-5}
Kerosine Oil	783	2090	0.15	2.1×10^{-6}

4.1.1 Governing Equations

For 3D incompressible steady fluid flow, boundary layer approximations are used, the above equations (4.1), (4.2), and (4.5) are reduced to:

$$U_x + V_y + W_z = 0, \tag{4.6}$$

$$UU_x + VU_y + WU_z = \upsilon_{hnf} U_{zz} + \frac{\sigma_{hnf}.B_0^2[-V\beta_e + U(1+\beta i\beta_e)]}{\rho_{hnf}\left[(1+\beta_e\beta i)^2 + (\beta_e)^2\right]}, \tag{4.7}$$

$$UV_x + VV_y + WV_z = \upsilon_{hnf} V_{zz} - \frac{\sigma h_{nf}.B_0^2[U\beta_e + V(1+\beta i\beta_e)]}{\rho h_{nf}\left[(1+\beta_e\beta i)^2 + (\beta_e)^2\right]}, \tag{4.8}$$

$$\begin{aligned} UT_x + VT_y + WT_z &= \frac{K_{hnf}}{(\rho C_p)_{hnf}} T_{zz} - \frac{\tau_o}{(\rho C_p)_{hnf}}\{W^2 T_{zz} + \\ &\quad (UW_x + VW_y + WW_z)T_z\} + \frac{Q}{(\rho C_p)_{hnf}}, \end{aligned} \tag{4.9}$$

where Q is the heat absorption/generation parameter and is given below

$$Q = [\frac{k_{hnf} U_w}{\nu_{hnf}(x+y)}\{A_1(T - T_\infty) + B_2(T_w - T_\infty)\}], \tag{4.10}$$

with associated boundary conditions

$$\begin{aligned} U|_{z=0} &= b(y+x), \qquad V|_{z=0} = c(y+x), \qquad W|_{z=0} = 0, T|_{z=0} = T_w, \\ U|_{z\to\infty} &= 0, \quad T|_{z\to\infty} = T_\infty. \end{aligned} \tag{4.11}$$

4.1.2 Similarity Transformation:

Following transformation is used to convert PDE's to ODE's:

$$\begin{aligned} u &= b(x+y)F'(\eta), \qquad v = b(x+y)G'(\eta), \quad w = -(bv_f)^{1/2}[F(\eta)+G(\eta)] \ , \\ \eta &= (b/v_f)^{1/2}z, \quad T = (T_w - T_\infty)\theta(\eta) + T_\infty. \end{aligned} \tag{4.12}$$

Using similarity transformations, the equation of continuity is identically satisfied, and the ordinary linear non-dimensional system of equations, including boundary conditions, has the following form:

$$(\frac{1}{\epsilon_1})F''' + F''(F+G) = F'(F'+G')] + (Ha)^2(\frac{\epsilon_2}{\epsilon_1})\{\frac{(1+\beta e\beta_i)F' - \beta_e G'}{(1+\beta_e\beta_i)^2+\beta_e^2}\}, \tag{4.13}$$

$$(\frac{1}{\epsilon_1})G''' + G''(F+G) = G'(F'+G')] + (Ha)^2(\frac{\epsilon_2}{\epsilon_1})\{\frac{(1+\beta e\beta_i)G' - \beta_e F'}{(1+\beta_e\beta_i)^2+\beta_e^2}\}, \tag{4.14}$$

$$(\frac{1}{\epsilon_3}\frac{k_{hnf}}{k_f})\theta''\frac{1}{\mathrm{Pr}} = [\gamma\{(F+G)^2\theta'' + (F+G)(F'+G')\theta' - (F+G)\theta'\}] + \frac{1}{\mathrm{Pr}}(A_1F' + B_2\theta). \tag{4.15}$$

where

$$\begin{aligned} \epsilon_1 &= (1-\phi_1)^{2.5}(1-\phi_2)^{2.5}(1-\phi_2)\{(1-\phi_1) + \phi_1\frac{\rho_{s1}}{\rho_f}\} + \phi_2\frac{\rho_{s2}}{\rho_f}, \\ \epsilon_2 &= ((1-\phi_1)^{2.5}(1-\phi_2)^{2.5}\{1 \\ &\quad + \frac{3\phi(\sigma_1\phi_1 + \sigma_2\phi_2 - \sigma_{bf}(\phi_1+\phi_2))}{[(\sigma_1\phi_1+\sigma_2\phi_2+2\phi\sigma_{bf}) - \phi\sigma_{bf}((\sigma_1\phi_1+\sigma_2\phi_2) - \sigma_{bf}(\phi_1+\phi_2))]}\}, \\ \epsilon_3 &= (1-\phi_2)\{(1-\phi_1) + \phi_1\frac{(\rho C_p)_{s1}}{(\rho C_p)_f}\} + \phi_2\frac{(\rho C_p)_{s2}}{(\rho C_p)_f}. \end{aligned} \tag{4.16}$$

with boundary conditions

$$F(0) = G(0) = 0, \quad F'(0) = 1, \quad G'(0) = a, \quad \theta(0) = 1 \quad F'(\infty) = G'(\infty) = \theta(\infty) = 0. \tag{4.17}$$

The expression for the non-dimensional parameter given in equation (4.13)-(4.15) are:

$$a = \frac{c}{b},\ Ha = (\frac{\sigma_{nf} B_o^2}{b\rho_f})^{\frac{1}{2}},\ \ \mathrm{Pr} = \frac{\mu_f (C_p)_f}{k_f},\ \gamma = \tau_o b. \tag{4.18}$$

Table 4.2: Model for nanofluid thermophysical properties

$k_{hnf} = \frac{k_{s_2}+2k_{bf}-2\varphi_2(k_{bf}-ks_2)}{k_{s_2}+2k_{bf}+\varphi_2(k_{bf}-ks_2)} \times k_{bf},$
$k_{bf} = \frac{k_{s_1}+2k_{bf}-2\varphi_1(k_{bf}-ks_1)}{k_{s1}+2k_{bf}+\varphi_2(k_{bf}-ks_1)} \times k_f,$
$\rho_{hnf} = \varphi_2\rho_{s_2} + (1-\varphi_2)\{(\varphi_1)\rho_{s_1} + (1-\varphi_1)\rho_f\},$
$\mu_{hnf} = \frac{\mu_f}{(1-\varphi_1)^{2.5}(1-\varphi_2)^{2.5}},$
$\alpha_{hnf} = \frac{k_{hnf}}{(\rho C_p)_{hnf}},$
$(\rho C_p)_{hnf} = (1-\phi_2)(\rho C_p)_f[(1-\phi_1) + \phi_1(\rho C_p)_{s_1} + \phi_2(\rho C_p)_{s_2}$
$\frac{\sigma_{hnf}}{\sigma_{bf}} = 1 + \frac{3\phi(\sigma_1\phi_1+\sigma_2\phi_2-\sigma_{bf}(\phi_1+\phi_2))}{[(\sigma_1\phi_1+\sigma_2\phi_2+2\phi\sigma_{bf})-\phi\sigma_{bf}((\sigma_1\phi_1+\sigma_2\phi_2)-\sigma_{bf}(\phi_1+\phi_2))]}\}.$

Dimensional form of Surface drag co-efficient and Nusselt number are

$$C_X = \frac{\tau_{xz}}{\rho_{hnf}.U^2}, \qquad C_Y = \frac{\tau_{yz}}{\rho_{hnf}.V^2}, \qquad Nu = \frac{(y+x)q_w}{(T_w - T_\infty)}, \tag{4.19}$$

$$\tau_{xz} = \mu_{hnf}(U_z + W_x)|_{z=0,} \qquad \tau_{yz} = \mu_{hnf}(V_z + W_y)|_{z=0}, \tag{4.20}$$

where q_w is heat flux near the wall, shear stress in x- and y-direction are τ_{xz} and τ_{yz} . The Nusselt and Skin drag coefficient has a non-dimensional form.

$$\begin{aligned} (\mathrm{Re}_{x_L})^{0.5} C_{Fx} &= \mu_{hnf} = \frac{1}{\epsilon_1} F''(0), \\ (\mathrm{Re}_{y_L})^{0.5} C_{G_y} &= \mu_{hnf} = \frac{1}{\epsilon_1} G''(0), \\ (\mathrm{Re})^{0.5} Nu_x &= -\frac{k_{hnf}}{k_f}\theta'(0) \end{aligned} \tag{4.21}$$

4.2 Numerical Solution

For a better understanding of the given problem, the non-linear system of differential equations is numerically solved. The Finite difference default method of bvp4c built in function of MATLAB scheme is used to evaluate the numerical results of equation (4.13-4.15) with boundary conditions (4.16). Tolerance is considered in this issue is 10^{-6}. By using the following numerical code,we get ODE's of order one.

$$\begin{aligned} y_1 &= F, \quad y_2 = F^{'}, \quad y_3 = F^{''}, \quad y_4 = G, \quad y_5 = G^{'}, \quad y_6 = G^{''}, \\ y_7 &= \theta, \quad y_8 = \theta^{'}, \quad yy_1 = F^{'''}, \quad yy_2 = G^{'''}, \quad yy_3 = \theta^{''}. \end{aligned} \tag{4.22}$$

$$\begin{aligned} yy_1 &= \epsilon_1[\{y(2)+y(5)\}y(2) - \{y(1)+y(4)\}y(3)) \\ &\quad +(\frac{\epsilon_2}{\epsilon 1})(Ha)^2\{\frac{(1+\beta_e\beta i)y(2)-\beta_e y(5))}{(1+(\beta_e\beta_i)^2+\beta_e^2)}], \end{aligned} \tag{4.23}$$

$$\begin{aligned} yy_2 &= \epsilon_1[\{y(2)+y(5)\}y(5) - \{y(1)+y(4)\}y(6)) \\ &\quad +(\frac{\epsilon_2}{\epsilon 1})(Ha)^2\{\frac{(1+\beta_e\beta i)y(5)-\beta_e y(2))}{(1+(\beta_e\beta_i)^2+\beta_e^2)}], \end{aligned} \tag{4.24}$$

$$\begin{aligned} yy_3 &= \frac{\Pr[\gamma\{y(1)+y(4)\}\{y(2)+y(5)\}y(8))] - \Pr\{y(1)+y(4)\}y(8)}{\frac{1}{\epsilon_3}\frac{k_{hnf}}{k_f} - \Pr\gamma\{y(1)+y(4)\}^2} \\ &\quad +\frac{1}{\Pr}(A_1 y(2) + B_2 y(7)), \end{aligned} \tag{4.25}$$

with B.C's

$$y_1(0) = y_4(0) = 0,\ y_2(0) = 1,\ y_5(0) = \lambda,\ y_7(0) = 1,\ y_2(\infty) = y_5(\infty) = y_7(\infty) = 0$$

4.3 Results and discussion

An exhaustive examination is directed to evaluate the impacts of ϕ_1, ϕ_2 β_i, β_e,$\gamma$and θ on velocity profile through Figs. 4.2 to 4.14. Figures 4.2 and 4.3 illustrate the change of $a = (c/b)$ on the $x-$ and $y-$velocity components, which are the ratio of the rate of stretched surface c in the y-direction to the rate of stretched surface in the x-direction. As a result, velocity is rising in the y direction while reducing in the x direction. The y-axis of momentum diffusion is greater than the x-axis of momentum diffusion. The association of Hall parameter with the fluid velocity in x and y-direction is portrayed in Figs. 4.4 and 4.5. It is evident in Fig. 4.4 that if the hall parameter increases, the movement of magnetized partially ionized liquid in the x-direction is enhanced. The product of electron collision time and their respective frequency is known as the Hall parameter. An increase in any one or both of these two boosts the Hall parameter resulting in Hall current known as Hall force. Hall and magnetic forces are opposite to each other. Consequently, for an increase in the Hall parameter, an increase in the velocity of the fluid in the x-direction. Similar behavior in the y-direction is seen. Fig. 4.6 delineates that velocity of nanofluid increases when β_i is expanded. In Fig. 4.7 similar impacts of the Hall and ion slip parameter on the hybrid nanofluid velocities along x- and y-directions are observed. The decreasing trend of the stretching ratio parameter on fluid temperature is depicted in Fig. 4.8. An increase in the linearly stretched parameter a causes an increase in the temperature, concentration, and nanoparticle concentration of nanofluid, resulting in a decrease in the heat, regular, and nano-mass transfer rates between the surface and the nanofluid. Figures 4.9 and 4.10 show studies of the impact of the Hall paramter and Ion slip parameter on partially ionized fluid temperature. A rise in these parameters causes the partially ionized fluid temperature to decrease. The thermal relaxation parameter decreases the fluid's heat transfer rate, and as a result, the temperature field decreases, as illustrated in Figs.4.11. The dynamic of fluid temperature for nanoparticle volume fractions is shown in Fig. 4.12(a,b). In the two different types of partially ionized liquids, hybrid nanoparticles are dispersed. The effectiveness of thermal conductivity is improved

as a result of nanoparticle dispersion in the mixture. Figs. 4.13(a,b) and 4.14(a,b) show the effect of a non-uniform heat generation/absorption parameter on the temperature field. Because of the non-uniform heat generation/absorption, the temperature of ionised hybrid nanofluid is dramatically raised. Higher non-uniform heat generation/absorption estimates generate more heat, which finally raises the fluid temperature. Lower non-uniform heat generation/absorption estimates absorbs more heat, which finally reduces the fluid temperature.

Temperature profiles are organized to investigate the temperature profile for change in ϕ, β_i, β_e,γ,$A_1$and B_2 and uncover that temperature of nanofluid diminishes by expanding volume capacity of nanoparticles. Such decline is the critical factor behind the use of nanomaterials in various electronic gadgets as a cooling agent. Truly an improvement in volume part of strong nanoparticles upgrades the viable conductivity of base fluid (water). Expansion in a diminishes the temperature of mixture nanofluid. This fact indicates that Hall current repulses any adjustment of fluid's temperature happened by the applied attractive field.

The effects of various factors on the rate of heat transfer and skin drag are shown in a table. The table illustrates numeric values for heat flux and skin drag for two types of partially ionized fluids (water and kerosene oil) versus two types of nanoparticles volume fraction φ, Hartmann number Ha, thermal time relaxation parameter γ, Hall and ion slip parameters β_e and βi and stretching ratio parameter a for two types of partially ionised fluids (water and kerosene oil).When the Hall parameter is raised, shear stress at the wall in the x-axis reduces, but shear stress at the wall rises when the ion slip parameter is enhanced. When the Hall parameter β_e is raised, shear stress at the wall reduces in the y-axis, but shear stress at the wall rises when the ion slip parameter is enhanced. When βi is increased, the heat flow at the wall increases. Numerical studies show that raising the thermal time relaxation parameter causes a modest increase in wall heat flux. When nanoparticle dispersion is enhanced, skin friction (both in the x and y axis) and heat flow at the wall increases. A comparison of the outcomes is depicted in special cases

with already published work Grubka and Bobba (1985) and Ishak et al. (2006) is given in Table 5.

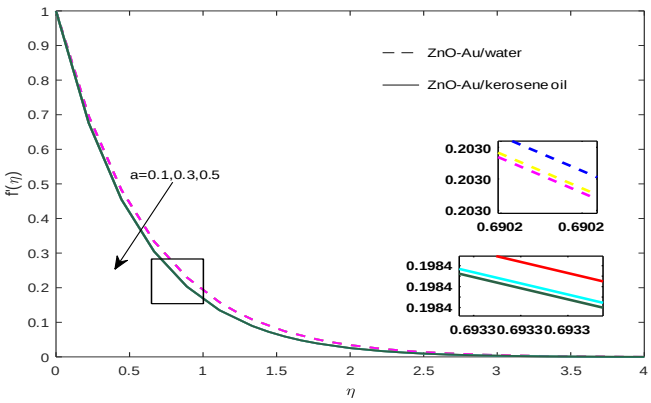

Fig. 4.2 Change in f′ (η) vs a

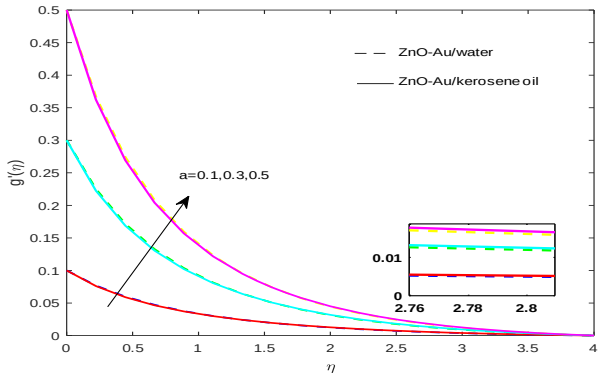

Fig. 4.3 Change in g′ (η) vs a

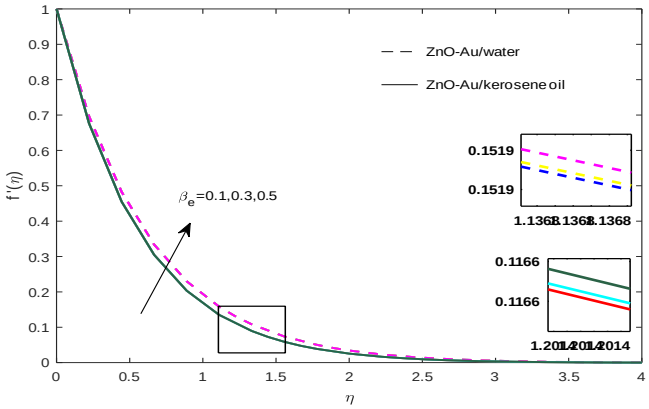

Fig. 4.4 Change in f′ (η) vs β_e

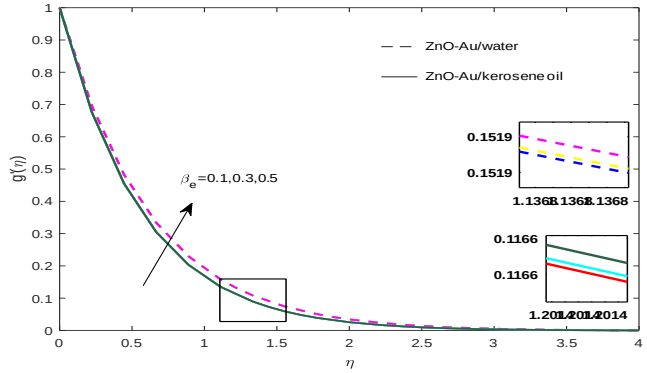

Fig. 4.5 Change in g′ (η) vs β_e

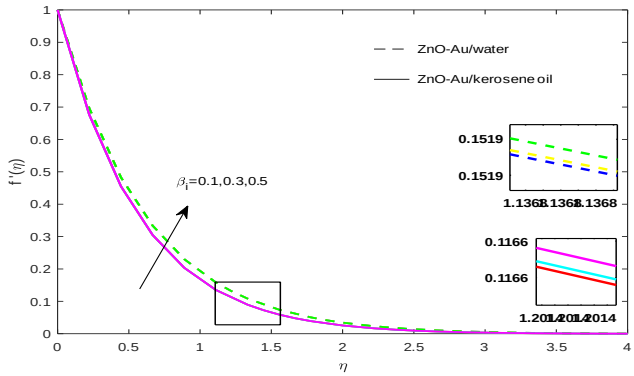

Fig. 4.6 Change in f′ (η) vs β_i

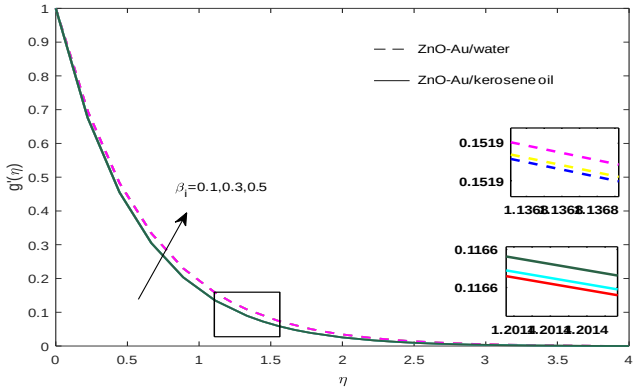

Fig. 4.7 Change in g′ (η) vs β_i

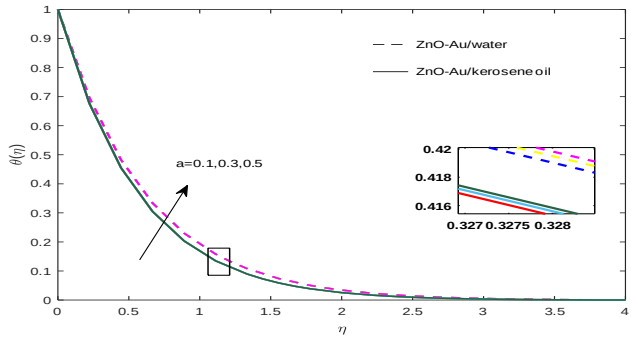

Fig. 4.8 Change in $\theta(\eta)$ vs a

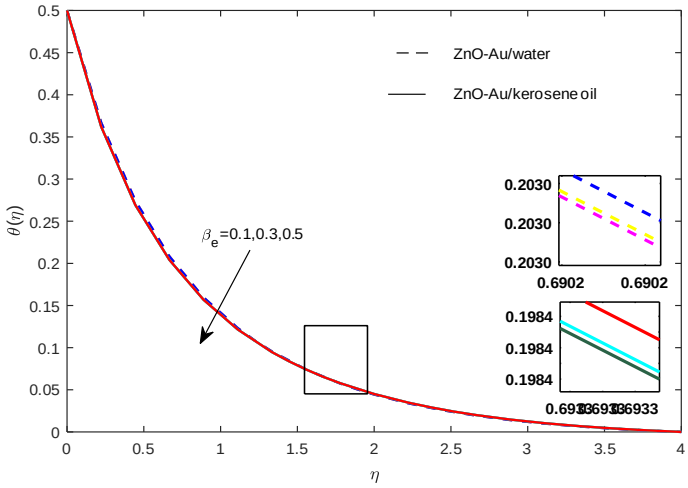

Fig. 4.9 Change in $\theta\,(\eta)$ vs β_e

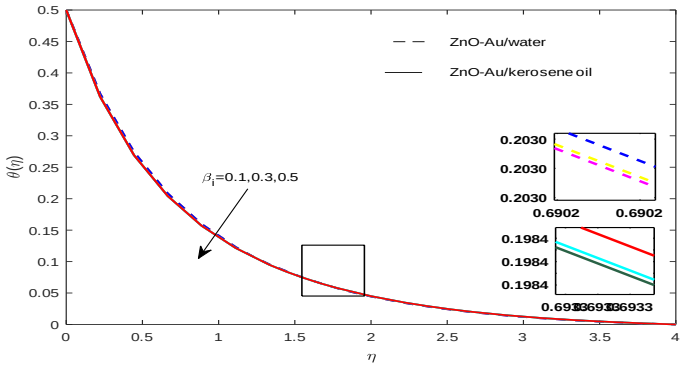

Fig. 4.10 Change in $\theta\,(\eta)$ vs β_i

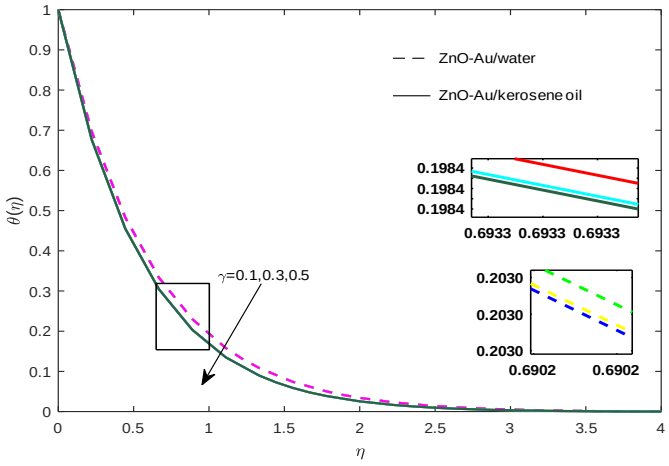

Fig. 4.11 Change in $\theta(\eta)$ vs γ

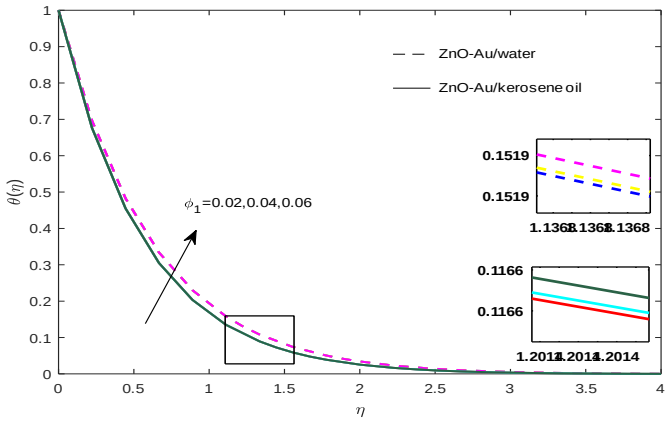

Fig. 4.12(a) Change in $\theta(\eta)$ vs ϕ_1

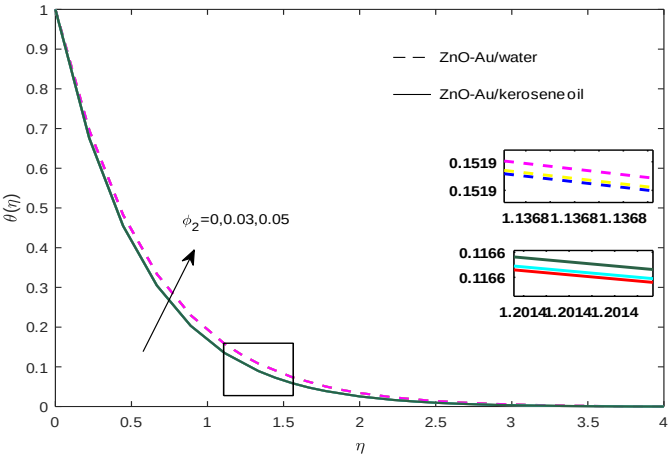

Fig. 4.12(b) Change in $\theta(\eta)$ vs ϕ_2

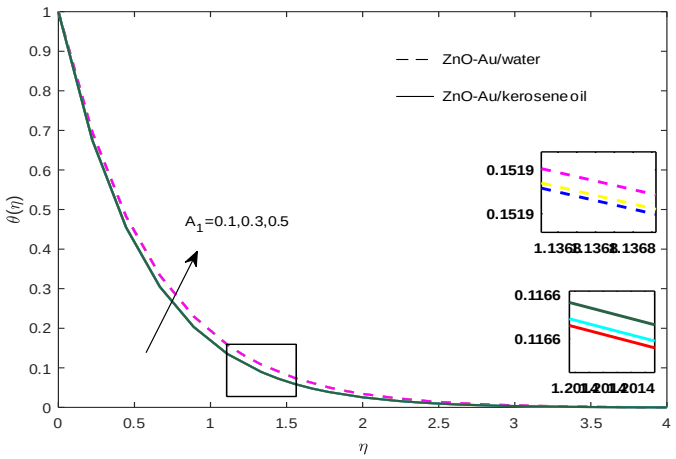

Fig. 4.13(a) Change in $\theta(\eta)$ vs A_1

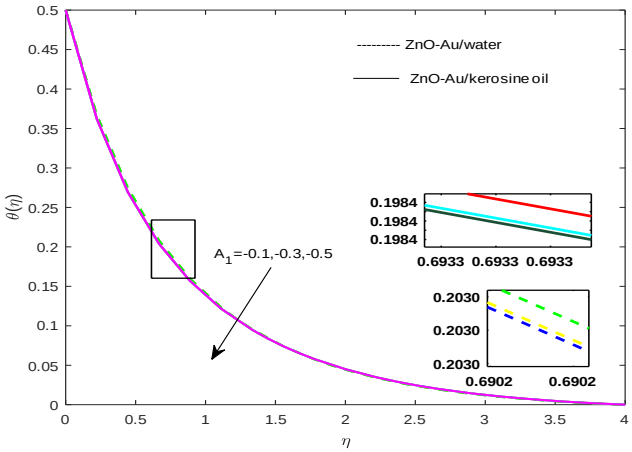

Fig. 4.13(b) Change in $\theta\,(\eta)$ vs A_1

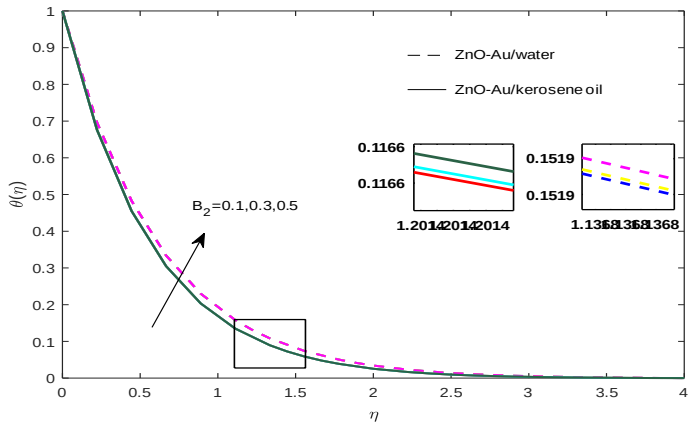

Fig. 4.14(a) Change in $\theta(\eta)$ vs B_2

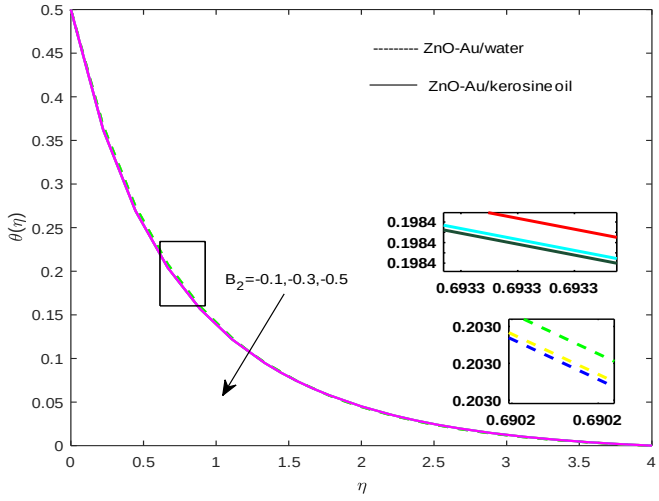

Fig. 4.14(b) Change in $\theta(\eta)$ vs B_2

Table 4.1 Analysis of surface drag in x-direction

φ_1	Ha	γ	β_e	β_i	a	Zno(water)	Au(water)	ZnO(oil)	Au(oil)
0.01						-0.3478952	-0.3612856	-0.3290680	-0.3468623
0.02						-0.2809354	-0.3045165	-0.2483745	-0.279019
0.03						-0.2209122	-0.2522615	-0.1782113	-0.2180605
0.01	0.1					-0.1690065	-0.1815156	-0.1558839	-0.1716080
	0.3					-0.1931705	-0.2065709	-0.1792828	-0.1960799
	0.5					-0.2399456	-0.2528109	-0.2240452	-0.2411975
	0.8	0.1				-0.3478952	-0.3612856	-0.3290680	-0.3471201
		0.3				-0.3478952	-0.3612856	-0.3290680	-0.3471201
		0.5				-0.3478952	-0.3612856	-0.3290680	-0.3471201
		0.5	0.1			-0.3652991	-0.3787380	-0.3460022	-0.3639729
			0.3			-0.3659952	-0.3612856	-0.3290680	-0.3468623
			0.5			-0.3670789	-0.3609839	-0.3264790	-0.3443249
			0.5	0.1		-0.3602233	-0.3736169	-0.3410002	-0.3589029
				0.3		-0.3537355	-0.3671276	-0.3347209	-0.3525666
				0.5		-0.3478952	-0.3612856	-0.3290680	-0.3468623
				0.5	0.1	-0.2289698	-0.2405280	-0.2105855	-0.2267139
					0.3	-0.2899924	-0.3024977	-0.2713945	-0.2885132
					0.5	-0.3478952	-0.3612856	-0.3290680	-0.3468623

Table 4.2 Analysis of surface drag in y-direction

φ_1	Ha	γ	β_e	β_i	a	ZnO(water)	Au(water)	ZnO(oil)	Au(oil)
0.01						-0.7481555	-0.7549908	-0.7366010	-0.7462150
0.02						-0.7090244	-0.7208294	-0.6891233	-0.7053459
0.03						-0.6741528	-0.6895493	-0.6481502	-0.6688613
0.01	0.1					-0.5861337	-0.5923779	-0.5795261	-0.5873872
	0.3					-0.6094333	-0.6161330	-0.6020764	-0.6105802
	0.5					-0.6529924	-0.6596934	-0.6442662	-0.6531216
	0.8	0.1				-0.7481555	-0.7549908	-0.7366010	-0.7463125
		0.3				-0.7481555	-0.7549908	-0.7366010	-0.7463125
		0.5				-0.7481555	-0.7549908	-0.7366010	-0.7463125
		0.5	0.1			-0.7094796	-0.7162494	-0.6990055	-0.7083001
			0.3			-0.7481555	-0.7549908	-0.7366010	-0.7462150
			0.5			-0.8043621	-0.8113016	-0.7911882	-0.8013409
			0.3	0.1		-0.7690649	-0.7759392	-0.7569085	-0.7667223
				0.3		-0.7578884	-0.7647415	-0.7460530	0.7557598
				0.5		-0.7481555	-0.7549908	-0.7366010	-0.7462150
				0.5	0.1	-0.1887964	-0.1900994	-0.1851113	-0.1873405
					0.3	-0.4546673	-0.4585576	-0.4471607	-0.4529255
					0.5	-0.7481554	-0.7549908	-0.7366010	-0.7462150

Table 4.3 The rate of heat transfer analysis

φ_1	Ha	γ	β_e	β_i	a	ZnO(water)	Au(water)	ZnO(oil)	Au(oil)
0.01						7.62571480	6.74610810	7.39028910	6.77532020
0.02						7.40456490	6.56191800	7.19080400	6.64042350
0.03						7.20172010	6.38516550	7.01120300	6.51230990
0.01	0.1					8.84063250	8.09590100	8.64775540	8.09759640
	0.3					8.56562160	7.80225640	8.35315670	7.81075800
	0.5					8.24252840	7.44828030	8.02300550	7.46420840
	0.8	0.1				7.62415740	6.68397270	7.38823010	6.70226120
		0.3				7.62415060	6.71482800	7.38225900	6.73769510
		0.5				7.62562480	6.74610810	7.39028910	6.77532020
		0.5	0.1			7.6968580	6.82813970	7.46333790	6.85591820
			0.3			7.62570480	6.74610810	7.39028910	6.77532020
			0.5			7.43556690	6.52417060	7.19450440	6.55655470
			0.3	0.1		7.53355578	6.63861360	7.29534810	6.66929950
				0.3		7.58225670	6.69550880	7.34553490	6.72542900
				0.5	0.1	7.62570480	6.74610810	7.39128920	6.77532020
					0.3	6.51155540	5.34888110	6.22776550	5.37534120

Chapter 5

Conclusions and future work

In this thesis the first problem is review work and second problem is about extension work , which has been analyzed . The following are the conclusions of both problems :-

5.1 Chapter 3

Three-dimensional comparative heat transfer research of two partially ionised fluids (water and kerosene oil) over a three-dimensional stretched sheet using two different nanoparticles (Cu and CuO). The impacts of Cu-nanoparticles have been described in this theoretical study.

- The temperature is higher when Cu-nanoparticles are distributed in slightly ionised water base fluid owing to the impacts of significant characteristics than the other three partially ionised nanofluids stated.
- CuO-water nanofluid has a higher partially ionised fluid velocity than the other nanofluids when velocity increases, while Cu-kerosene oil nanofluid has a considerable decline in fluid velocity when velocity decreases.
- CuO nanoparticles dispersed in the base for better thermal efficiency; fluid kerosene oil other than partially ionised water fluid is suggested for observance.

5.2 Chapter 4

The flow of a hybrid nanofluid containing ZnO and Au nanoparticles imbedded in two different partically ionised liquids (water and kerosene oil) over a 3D stretched sheet is studied. The subject flow is influenced by the Hall and Ion slip impacts with the non uniform heat source/sink.

- As the stretching parameter is increased, the heat transfer rate of the hybrid nanofluid increases.
- The impact of Ion slip parameter β_i on velocity field is more significant in the x-direction as compared to the velocity in y-direction.
- Prandtl number shows decreasing trend against temperature.
- Thermal relaxaion coefficient γ has a decreasing effect on temperature profile $\theta(\eta)$.
- By increasing the heat generation parameter, the thermal boundary of the hybrid nanofluid expands.
- Hybridity boosts the temperature distribution as well as the heat transfer rate at surface.

5.3 Chapter 5

As the future works, it is suggested that the present research work would be accomplished with other nanoparticles (mettalic or non-mettalic) as well as with various base fluids.

Bibliography

[1] Wong, K. V., & De Leon, O. (2010). Applications of nanofluids: current and future. Advances in mechanical engineering, 2, 519659.

[2] Kostic, M. M. (2013). Critical issues in nanofluids research and application potentials. Nova Science Publishers, 1-49.

[3] Eastman, J. A., Choi, S. U. S., Li, S., Yu, W., & Thompson, L. J. (2001). Anomalously increased effective thermal conductivities of ethylene glycol-based nanofluids containing copper nanoparticles. Applied physics letters, 78(6), 718-720.

[4] Eastman, J. A., Choi, U. S., Li, S., Thompson, L. J., & Lee, S. (1996). Enhanced thermal conductivity through the development of nanofluids. MRS Online Proceedings Library (OPL), 457.

[5] Choi, S. U., & Eastman, J. A. (1995). Enhancing thermal conductivity of fluids with nanoparticles (No. ANL/MSD/CP-84938; CONF-951135-29). Argonne National Lab., IL (United States).

[6] Tiwari, R. K., & Das, M. K. (2007). Heat transfer augmentation in a two-sided lid-driven differentially heated square cavity utilizing nanofluids. International Journal of heat and Mass transfer, 50(9-10), 2002-2018.

[7] Kuznetsov, A. V., & Nield, D. A. (2010). Natural convective boundary-layer flow of a nanofluid past a vertical plate. International Journal of Thermal Sciences, 49(2), 243-247.

[8] Khan, W. A., & Aziz, A. (2011). Natural convection flow of a nanofluid over a vertical plate with uniform surface heat flux. International Journal of Thermal Sciences, 50(7), 1207-1214.

[9] Buongiorno, J. (2006). Convective transport in nanofluids.

[10] Kakaç, S., & Pramuanjaroenkij, A. (2009). Review of convective heat transfer enhancement with nanofluids. International journal of heat and mass transfer, 52(13-14), 3187-3196.

[11] Khan, W. A., & Pop, I. (2010). Boundary-layer flow of a nanofluid past a stretching sheet. International journal of heat and mass transfer, 53(11-12), 2477-2483.

[12] Rana, P., & Bhargava, R. (2012). Flow and heat transfer of a nanofluid over a nonlinearly stretching sheet: a numerical study. Communications in Nonlinear Science and Numerical Simulation, 17(1), 212-226.

[13] Van Gorder, R. A., Sweet, E., & Vajravelu, K. (2010). Nano boundary layers over stretching surfaces. Communications in Nonlinear Science and Numerical Simulation, 15(6), 1494-1500.

[14] Hassani, M., Tabar, M. M., Nemati, H., Domairry, G., & Noori, F. (2011). An analytical solution for boundary layer flow of a nanofluid past a stretching sheet. International Journal of Thermal Sciences, 50(11), 2256-2263.

[15] Akyildiz, F. T., Bellout, H., Vajravelu, K., & Van Gorder, R. A. (2011). Existence results for third order nonlinear boundary value problems arising in nano boundary layer fluid flows over stretching surfaces. Nonlinear Analysis: Real World Applications, 12(6), 2919-2930.

[16] Turcu, R., Darabont, A. L., Nan, A., Aldea, N., Macovei, D., Bica, D., ... & Biro, L. P. (2006). New polypyrrole-multiwall carbon nanotubes hybrid materials. Journal of optoelectronics and advanced materials, 8(2), 643-647.

[17] Jana, S., Salehi-Khojin, A., & Zhong, W. H. (2007). Enhancement of fluid thermal conductivity by the addition of single and hybrid nano-additives. Thermochimica acta, 462(1-2), 45-55.

[18] Sarkar, J., Ghosh, P., & Adil, A. (2015). A review on hybrid nanofluids: recent research, development and applications. Renewable and Sustainable Energy Reviews, 43, 164-177.

[19] Esfe, M. H., Alirezaie, A., & Rejvani, M. (2017). An applicable study on the thermal conductivity of SWCNT-MgO hybrid nanofluid and price-performance analysis for energy management. Applied Thermal Engineering, 111, 1202-1210.

[20] Rostami, S., Nadooshan, A. A., & Raisi, A. (2020). The effect of hybrid nano-additive consists of graphene oxide and copper oxide on rheological behavior of a mixture of water and ethylene glycol. Journal of Thermal Analysis and Calorimetry, 139(3), 2353-2364.

[21] Taherialekouhi, R., Rasouli, S., & Khosravi, A. (2019). An experimental study on stability and thermal conductivity of water-graphene oxide/aluminum oxide nanoparticles as a cooling hybrid nanofluid. International Journal of Heat and Mass Transfer, 145, 118751.

[22] Kaska, S. A., Khalefa, R. A., & Hussein, A. M. (2019). Hybrid nanofluid to enhance heat transfer under turbulent flow in a flat tube. Case Studies in Thermal Engineering, 13, 100398.

[23] Al-Mdallal, Q. M., Indumathi, N., Ganga, B., & Hakeem, A. A. (2020). Marangoni radiative effects of hybrid-nanofluids flow past a permeable surface with inclined magnetic field. Case Studies in Thermal Engineering, 17, 100571.

[24] Waini, I., Ishak, A., & Pop, I. (2020). Transpiration effects on hybrid nanofluid flow and heat transfer over a stretching/shrinking sheet with uniform shear flow. Alexandria Engineering Journal, 59(1), 91-99.

[25] Aladdin, N. A. L., Bachok, N., & Pop, I. (2020). Cu-Al2O3/water hybrid nanofluid flow over a permeable moving surface in presence of hydromagnetic and suction effects. Alexandria Engineering Journal, 59(2), 657-666.

[26] Khan, U., Zaib, A., & Mebarek-Oudina, F. (2020). Mixed convective magneto flow of SiO 2–MoS 2/C 2 H 6 O 2 hybrid nanoliquids through a vertical stretching/shrinking wedge: stability analysis. Arabian Journal for Science and Engineering, 45, 9061-9073.

[27] Hamrelaine, S., Mebarek-Oudina, F., & Sari, M. R. (2019). Analysis of MHD Jeffery Hamel flow with suction/injection by homotopy analysis method. Journal of Advanced Research in Fluid Mechanics and Thermal Sciences, 58(2), 173-186.

[28] Marzougui, S., Mebarek-Oudina, F., Assia, A., Magherbi, M., Shah, Z., & Ramesh, K. (2021). Entropy generation on magneto-convective flow of copper–water nanofluid in a cavity with chamfers. Journal of Thermal Analysis and Calorimetry, 143(3), 2203-2214.

[29] Raza, J., Mebarek-Oudina, F., Ram, P., & Sharma, S. (2020). MHD flow of non-Newtonian molybdenum disulfide nanofluid in a converging/diverging channel with Rosseland radiation. In Defect and Diffusion Forum (Vol. 401, pp. 92-106).

[30] Farhan, M., Omar, Z., Mebarek-Oudina, F., Raza, J., Shah, Z., Choudhari, R. V., & Makinde, O. D. (2020). Implementation of the one-step one-hybrid block method on the nonlinear equation of a circular sector oscillator. Computational Mathematics and Modeling, 31(1), 116-132.

[31] Mebarek-Oudina, F. (2019). Convective heat transfer of Titania nanofluids of different base fluids in cylindrical annulus with discrete heat source. Heat Transfer—Asian Research, 48(1), 135-147.

[32] Raza, J., Farooq, M., Mebarek-Oudina, F., & Mahanthesh, B. (2019). Multiple slip effects on MHD non-Newtonian nanofluid flow over a nonlinear permeable elongated

sheet: numerical and statistical analysis. Multidiscipline Modeling in Materials and Structures.

[33] Gul, N., Ramzan, M., Chung, J. D., Kadry, S., & Chu, Y. M. (2020). Impact of hall and ion slip in a thermally stratified nanofluid flow comprising Cu and Al 2 O 3 nanoparticles with nonuniform source/sink. Scientific Reports, 10(1), 1-18.

[34] Nawaz, M., Hayat, T., & Alsaedi, A. (2013). Mixed convection three-dimensional flow in the presence of hall and ion-slip effects. Journal of heat transfer, 135(4).

[35] Ramzan, M., Ullah, N., Chung, J. D., Lu, D., & Farooq, U. (2017). Buoyancy effects on the radiative magneto Micropolar nanofluid flow with double stratification, activation energy and binary chemical reaction. Scientific reports, 7(1), 1-15.

[36] Ramzan, M., Gul, H., Chung, J. D., Kadry, S., & Chu, Y. M. (2020). Significance of Hall effect and Ion slip in a three-dimensional bioconvective Tangent hyperbolic nanofluid flow subject to Arrhenius activation energy. Scientific Reports, 10(1), 1-15.

[37] Nawaz, M., Rana, S., Qureshi, I. H., & Hayat, T. (2018). Three-dimensional heat transfer in the mixture of nanoparticles and micropolar MHD plasma with Hall and ion slip effects. AIP Advances, 8(10), 105109.

[38] Abid, N., Ramzan, M., Chung, J. D., Kadry, S., & Chu, Y. M. (2020). Comparative analysis of magnetized partially ionized copper, copper oxide–water and kerosene oil nanofluid flow with Cattaneo–Christov heat flux. Scientific Reports, 10(1), 1-14.

[39] Zeeshan, A., Bhatti, M. M., Muhammad, T., & Zhang, L. (2020). Magnetized peristaltic particle–fluid propulsion with Hall and ion slip effects through a permeable channel. Physica A: Statistical Mechanics and its Applications, 550, 123999.

[40] Ibrahim, W., & Anbessa, T. (2021). Hall and ion-slip effects on mixed convection flow of Williamson nanofluid over a nonlinear porous stretching sheet with variable thermal conductivity. Heat Transfer, 50(6), 5627-5651.

Maryam Thesis

ORIGINALITY REPORT

18%	9%	16%	%
SIMILARITY INDEX	INTERNET SOURCES	PUBLICATIONS	STUDENT PAPERS

PRIMARY SOURCES

1	Nomana Abid, Muhammad Ramzan, Jae Dong Chung, Seifedine Kadry, Yu-Ming Chu. "Comparative analysis of magnetized partially ionized copper, copper oxide–water and kerosene oil nanofluid flow with Cattaneo–Christov heat flux", Scientific Reports, 2020 Publication	3%
2	Jae Dong Chung, Muhammad Ramzan, Hina Gul, Nosheen Gul, Seifedine Kadry, Yu-Ming Chu. "Partially ionized hybrid nanofluid flow with thermal stratification", Journal of Materials Research and Technology, 2021 Publication	2%
3	www.ncbi.nlm.nih.gov Internet Source	2%
4	www.hindawi.com Internet Source	1%
5	www.unboundmedicine.com Internet Source	1%

6	Muhammad Shoaib, Muhammad Asif Zahoor Raja, Muhammad Touseef Sabir, Muhammad Awais, Saeed Islam, Zahir Shah, Poom Kumam. "Numerical analysis of 3-D MHD hybrid nanofluid over a rotational disk in presence of thermal radiation with Joule heating and viscous dissipation effects using Lobatto IIIA technique", Alexandria Engineering Journal, 2021 Publication	1 %
7	M. Ramzan, M. Bilal, Jae Dong Chung, Dian Chen Lu, Umer Farooq. "Impact of generalized Fourier's and Fick's laws on MHD 3D second grade nanofluid flow with variable thermal conductivity and convective heat and mass conditions", Physics of Fluids, 2017 Publication	1 %
8	A. Anjum, N.A. Mir, M. Farooq, M. Ijaz Khan, T. Hayat. "Influence of thermal stratification and slip conditions on stagnation point flow towards variable thicked Riga plate", Results in Physics, 2018 Publication	<1 %
9	www.preprints.org Internet Source	<1 %
10	iopscience.iop.org Internet Source	<1 %

11	Shafia Rana, M Nawaz, Mohammed Kbiri Alaoui. "Three dimensional heat transfer in the Carreau-Yasuda hybrid nanofluid with Hall and ion slip effects", Physica Scripta, 2021 Publication	<1 %
12	"Advances in Fluid Dynamics", Springer Science and Business Media LLC, 2021 Publication	<1 %
13	Kalidas Das. "Nanofluid flow over a non-linear permeable stretching sheet with partial slip", Journal of the Egyptian Mathematical Society, 2015 Publication	<1 %
14	Nosheen Gul, Muhammad Ramzan, Jae Dong Chung, Seifedine Kadry, Yu-Ming Chu. "Impact of hall and ion slip in a thermally stratified nanofluid flow comprising Cu and Al2O3 nanoparticles with nonuniform source/sink", Scientific Reports, 2020 Publication	<1 %
15	Muhammad Asif Zahoor Raja, Zeeshan Khan, Samina Zuhra, Naveed Ishtiaq Chaudhary et al. "Cattaneo-christov heat flux model of 3D hall current involving biconvection nanofluidic flow with Darcy-Forchheimer law effect: Backpropagation neural networks approach", Case Studies in Thermal Engineering, 2021 Publication	<1 %

16	Khan, Junaid Ahmad, M. Mustafa, T. Hayat, M. Sheikholeslami, and A. Alsaedi. "Three-Dimensional Flow of Nanofluid Induced by an Exponentially Stretching Sheet: An Application to Solar Energy", PLoS ONE, 2015. Publication	<1 %
17	prr.hec.gov.pk Internet Source	<1 %
18	Muhammad Ramzan, Hina Gul, Jae Dong Chung, Seifedine Kadry, Yu-Ming Chu. "Significance of Hall effect and Ion slip in a three-dimensional bioconvective Tangent hyperbolic nanofluid flow subject to Arrhenius activation energy", Scientific Reports, 2020 Publication	<1 %
19	link.springer.com Internet Source	<1 %
20	rigeo.org Internet Source	<1 %
21	Hajra Kaneez, M Nawaz, Mohammed Kbiri Alaoui, Zahra Abdelmalek. "An enhancement in transportation of heat energy in yield stress dusty fluid via mono and hybrid nanoparticles", Physica Scripta, 2020 Publication	<1 %
22	P. LOGANATHAN, P. NIRMAL CHAND, P. GANESAN. "RADIATION EFFECTS ON AN	<1 %

UNSTEADY NATURAL CONVECTIVE FLOW OF A NANOFLUID PAST AN INFINITE VERTICAL PLATE", Nano, 2013
Publication

23	pt.scribd.com Internet Source	<1 %
24	Monica Medikare, Sucharitha Joga, Kishore Kumar Chidem. "MHD Stagnation Point Flow of a Casson Fluid over a Nonlinearly Stretching Sheet with Viscous Dissipation", American Journal of Computational Mathematics, 2016 Publication	<1 %
25	N. Anbuchezhian, K. Srinivasan, K. Chandrasekaran, R. Kandasamy. "Thermophoresis and Brownian motion effects on boundary layer flow of nanofluid in presence of thermal stratification due to solar energy", Applied Mathematics and Mechanics, 2012 Publication	<1 %
26	S. Das, R. N. Jana, O. D. Makinde. "MHD Boundary Layer Slip Flow and Heat Transfer of Nanofluid Past a Vertical Stretching Sheet with Non-Uniform Heat Generation/Absorption", International Journal of Nanoscience, 2014 Publication	<1 %

27	nanoscalereslett.springeropen.com Internet Source	<1%
28	Iskandar Waini, Ioan Pop, Sakhinah Abu Bakar, Anuar Ishak. "Stagnation point flow toward an exponentially shrinking sheet in a hybrid nanofluid", International Journal of Numerical Methods for Heat & Fluid Flow, 2021 Publication	<1%
29	Bidyut Mandal, G. C. Layek. "Unsteady MHD mixed convective Casson fluid flow over a flat surface in the presence of slip", International Journal of Modern Physics C, 2020 Publication	<1%
30	Muhammad Bilal Hafeez, Rohul Amin, Kottakkaran Sooppy Nisar, Wasim Jamshed, Abdel-Haleem Abdel-Aty, M. Motawi Khashan. "Heat transfer enhancement through nanofluids with applications in automobile radiator", Case Studies in Thermal Engineering, 2021 Publication	<1%
31	T. Vijaya Laxmi, Bandari Shankar. "Effect of Nonlinear Thermal Radiation on Boundary Layer Flow of Viscous Fluid over Nonlinear Stretching Sheet with Injection/Suction", Journal of Applied Mathematics and Physics, 2016	<1%

Publication

32	scholarcommons.usf.edu Internet Source	<1 %
33	Basant K. Jha, Gabriel Samaila, Peter B. Malgwi. "Adomian decomposition method for combined effect of Hall and ion-slip on mixed convection flow of chemically reacting Newtonian fluid in a microchannel with heat absorption/generation", International Journal of Modern Physics C, 2020 Publication	<1 %
34	C. Igathinathane, V. K. Malleswar, U. Appa Rao, L. O. Pordesimo, A. R. Womac. "Viscosity Measurement Technique Using Standard Glass Burette for Newtonian Liquids", Instrumentation Science & Technology, 2005 Publication	<1 %
35	Das, Kalidas. "Slip flow and convective heat transfer of nanofluids over a permeable stretching surface", Computers & Fluids, 2012. Publication	<1 %
36	JAMES P. DENIER, PETER W. DUCK, JIAN LI. "On the growth (and suppression) of very short-scale disturbances in mixed forced–free convection boundary layers", Journal of Fluid Mechanics, 2005 Publication	<1 %

37	Tasawar Hayat, Sajid Qayyum, Sabir Ali Shehzad, Ahmed Alsaedi. "Magnetohydrodynamic three-dimensional nonlinear convection flow of Oldroyd-B nanoliquid with heat generation/absorption", Journal of Molecular Liquids, 2017 Publication	<1 %
38	Wubshet Ibrahim, Temesgen Anbessa. "Mixed convection flow of a Maxwell nanofluid with Hall and ion - slip impacts employing the spectral relaxation method", Heat Transfer, 2020 Publication	<1 %
39	repo.uum.edu.my Internet Source	<1 %
40	Hatice Mercan. "Thermophysical and rheological properties of hybrid nanofluids", Elsevier BV, 2020 Publication	<1 %
41	Hongtao Gao, Fei Mao, Yuchao Song, Jiaju Hong, Yuying Yan. "Chapter 42 Enhance Heat Transfer and Mass Transfer in the Falling Film Absorption Process by Adding Nanoparticles", Springer Science and Business Media LLC, 2021 Publication	<1 %

42	Khalil Ur Rehman, Noor Ul Saba, M. Y. Malik, Iffat Zehra. "Nanoparticles individualities in both Newtonian and Casson fluid models by way of stratified media: A numerical analysis", The European Physical Journal E, 2018 Publication	<1 %
43	Khan, Junaid Ahmad, Meraj Mustafa, Tasawar Hayat, and Ahmed Alsaedi. "On Three-Dimensional Flow and Heat Transfer over a Non-Linearly Stretching Sheet: Analytical and Numerical Solutions", PLoS ONE, 2014. Publication	<1 %
44	Mania Goyal, Rama Bhargava. "Numerical study of thermodiffusion effects on boundary layer flow of nanofluids over a power law stretching sheet", Microfluidics and Nanofluidics, 2014 Publication	<1 %
45	Wubshet Ibrahim, Temesgen Anbessa. "Hall and Ion Slip Effects on Mixed Convection Flow of Eyring-Powell Nanofluid over a Stretching Surface", Advances in Mathematical Physics, 2020 Publication	<1 %
46	Yu-Pei Lv, Hina Gul, Muhammad Ramzan, Jae Dong Chung, Muhammad Bilal. "Bioconvective Reiner–Rivlin nanofluid flow over a rotating disk with Cattaneo–Christov	<1 %

flow heat flux and entropy generation analysis", Scientific Reports, 2021
Publication

47	Zahoor Iqbal, Masood Khan, Awais Ahmed.. "Features of relaxation and retardation time constants in forced convective Burger's nanofluid flow subject to Cattaneo-Christov theory", The European Physical Journal Applied Physics, 2020 Publication	<1 %
48	mafiadoc.com Internet Source	<1 %
49	www.mori.cs.titech.ac.jp Internet Source	<1 %
50	"Engineering Mathematics I", Springer Science and Business Media LLC, 2016 Publication	<1 %
51	A.Kh. Khachatryan, Kh.A. Khachatryan. "A UNIQUENESS THEOREM FOR A NONLINEAR SINGULAR INTEGRAL EQUATION ARISING IN $ p $-ADIC STRING THEORY", Proceedings of the YSU A: Physical and Mathematical Sciences, 2019 Publication	<1 %
52	Bai Yu, Muhammad Ramzan, Saima Riasat, Seifedine Kadry, Yu-Ming Chu, M. Y. Malik. "Impact of autocatalytic chemical reaction in	<1 %

an Ostwald-de-Waele nanofluid flow past a rotating disk with heterogeneous catalysis", Scientific Reports, 2021
Publication

53 Dianchen Lu, M. Ramzan, Shafiq Ahmad, Jae Dong Chung, Umer Farooq. "Upshot of binary chemical reaction and activation energy on carbon nanotubes with Cattaneo-Christov heat flux and buoyancy effects", Physics of Fluids, 2017 <1 %
Publication

54 Gireesha, BJ, and NG Rudraswamy. "Chemical reaction on MHD flow and heat transfer of a nanofluid near the stagnation point over a permeable stretching surface with non-uniform heat source/sink", International Journal of Engineering Science and Technology, 2014. <1 %
Publication

55 Iskandar Waini, Anuar Ishak, Ioan Pop. "Hybrid nanofluid flow towards a stagnation point on an exponentially stretching/shrinking vertical sheet with buoyancy effects", International Journal of Numerical Methods for Heat & Fluid Flow, 2020 <1 %
Publication

56 Sanatan Das, Akram Ali, Rabindra Nath Jana. "Numerically framing the impact of magnetic <1 %

field on nanofluid flow over a curved stretching surface with convective heating", World Journal of Engineering, 2021
Publication

57	T. Hayat, M. Nawaz. "Soret and Dufour effects on the mixed convection flow of a second grade fluid subject to Hall and ion-slip currents", International Journal for Numerical Methods in Fluids, 2011 Publication	<1 %
58	Yonghong Shen, Faxing Wang. "Variable precision rough set model over two universes and its properties", Soft Computing, 2010 Publication	<1 %
59	archive.org Internet Source	<1 %
60	asmedigitalcollection.asme.org Internet Source	<1 %
61	commons.und.edu Internet Source	<1 %
62	jafmonline.net Internet Source	<1 %
63	tudr.thapar.edu:8080 Internet Source	<1 %
64	Hyeongmin Kim, Jinhyun Kim, Honghyun Cho. "Review of Thermal Performance and	<1 %

Efficiency in Evacuated Tube Solar Collector with Various Nanofluids", International Journal of Air-Conditioning and Refrigeration, 2017
Publication

---

65 M. Santhi, K. V. Suryanarayana Rao, Patakota Sudarsana Reddy, P. Sreedevi. "HEAT AND MASS TRANSFER ANALYSIS OF STEADY AND UNSTEADY NANOFLUID FLOW OVER A STRETCHING SHEET WITH DOUBLE STRATIFICATION", Nanoscience and Technology: An International Journal, 2019 <1 %
Publication

---

66 Nevine Michael. "Optoelectronic parallel watershed implementation for segmentation of magnetic resonance brain images", Applied Optics, 12/10/1997 <1 %
Publication

---

67 Wubshet Ibrahim, Temesgen Anbessa. "Three-Dimensional MHD Mixed Convection Flow of Casson Nanofluid with Hall and Ion Slip Effects", Mathematical Problems in Engineering, 2020 <1 %
Publication

---

68 M Nawaz, Uzma Arif, Imran Haider Qureshi. "Impact of temperature dependent diffusion coefficients on heat and mass transport in viscoelastic liquid using generalized Fourier theory", Physica Scripta, 2019 <1 %
Publication

Exclude quotes	On	Exclude matches	< 5 words
Exclude bibliography	On		